THE UNITED STATES PATENT AND TRADEMARK OFFICE

Art Unit	: 1733	Customer No. 035811
Examiner	: Mark L. Shevin	
Serial No.	: 10/587,807	Docket No.: JFE-06-1181
Filed	: July 28, 2006	
Inventors	: Yukio Miyata	Confirmation No.: 5332
	: Mitsuo Kimura	
	: Noritsugu Itakura	
	: Katsumi Masamura	
Title	: MARTENSITIC STAINLESS	
	: STEEL PIPE	

DECLARATION OF YUKIO MIYATA

Commissioner for Patents
P.O. Box 1450
Alexandria, VA 22313-1450

Sir:

I, Yukio Miyata, declare as follows:

I am one of the inventors named in the above-identified US Patent Application and am thoroughly familiar with the above-referenced patent application.

I reside in Aichi, Japan.

My educational background is summarized as follows:

April 1983: I entered the Fourth Course of Osaka University.

March 1987: I graduated from Osaka University.

April 1987: I entered the Graduate School of Engineering, Osaka University.

March 1989: I graduated from the Graduate School of Engineering, Osaka University.

My work experience is summarized as follows:

I was employed by Kawasaki Steel Corporation from April 1989 to 2003 as a material and corrosion researcher. I was engaged in research concerning the development of linepipe and OCTG.

After a merger to JFE Steel Corporation in April 2003, I have been employed by JFE Steel Corporation as a material and corrosion researcher continuously, wherein I have been engaged in the development of linepipe and OCTG.

I attach to this Declaration two sheets of Comparative Tables which have information on Examples taken from Kimura and Examples taken from JP '604. Those Examples show in the far right-hand column the amount of C_{eq} for each of those examples. In every case, the amount of C_{eq} is more than than the amount of C_{eq} that is claimed in this application.

The amount of C_{eq} in each instance was determined by utilizing the methodology which is also in the claims of this application, particularly the last portion of Claim 2.

I believe that the discovery that I and my co-inventors made is quite unexpected over the Kimura and JP '604 disclosures because they had no appreciation for our discovery that Cr carbides precipitate at the prior-austenite grain boundaries during welding thermal cycles, which results in the formation of Cr depleted zones around the prior-austenite grain boundaries which ultimately causes IGSCC.

I further believe that our discovery is unexpected over the Kimura and JP '604 publications because there is nothing in either disclosure that suggests the ability of preventing Cr carbide from being formed at those prior-austenite grain boundaries by limiting the C_{eq} content in the amount of less than or equal to 0.0050% as being claimed.

We believe that this unexpected and highly advantageous discovery has resulted in commercial notoriety and success which is linked to that discovery.

I also attach to this Declaration a copy of a newspaper article and an English translation thereof that shows the extremely successful sales result we achieved by our ability to commercially supply steels in accordance with our claims. As shown in the article, the previous

largest single sale of steel of this general type was 3,000 tons. However, this single sale was for 21,000 tons, namely seven times larger than the previous sale. This incredible sale of increase is directly attributable to the ability of these steels to prevent IGSCC.

I further enclose three additional excerpts which are English language literature pieces describing the highly advantageous features of our new steels. I therefore believe that this is further evidence that our claimed steels are not obvious over Kimura and JP '604.

The undersigned declares that all statements made herein of his own knowledge are true and that all statements made on information and belief are believed to be true; and further that these statements were made with the knowledge that willful false statements and the like so made are punishable by fine or imprisonment, or both, under Section 1001 of Title 18 of the United States Code and thus such willful false statements may jeopardize the validity of the application or any patent issuing thereon.

Date: October 31, 2011

Yukio Miyata

Yukio Miyata, Co-inventor

Comparative Table

outside the range of the amended claim 4

the range of the amended claim 4

		C	Si	Mn	P	S	Cr	Ni	Al	N	Mo	Cu	Co	W	Ti	Nb	V	Zr	Ca	Hf	Ta	Mg	REM	B	O	C-sol
	lower limit		0.05	0.1			10	3	0.001								0.02		0.0005							
	upper limit	below0.01	1.0	2.0	0.03	0.010	14	8	0.10	below0.01	4	4	4	4	0.15	0.10	0.10	0.10	0.010	0.20	0.20					0.0060

A:0859985209

	No.	C	Si	Mn	P	S	Cr	Ni	Al	N	Mo	Cu	Co	W	Ti	Nb	V	Zr	Ca	Hf	Ta	Mg	REM	B	O	C-sol
Tabl	1	0.010	0.25	0.44			12.10	3.86	0.02	0.024	1.02	0.49														0.0169
	2	0.014	0.25	0.47			12.9	4.06	0.02	0.047	0.95															0.0274
	3	0.013	0.24	0.45			13.1	1.15	0.02	0.025	0.52	0.50				0.047										0.0191
	4	0.005	0.25	0.45			12.2	5.12	0.02	0.010	2.02							0.016								0.0075
	5	0.009	0.25	0.44			10.7	1.47	0.02	0.015	1.55															0.0133
	6	0.008	0.23	0.46			11.2	1.18	0.02	0.023	0.91	0.51									0.031					0.0143
	7	0.014	0.21	0.51			11.0	0.80	0.02	0.031	1.47	0.24							0.002							0.0229
	8	0.016	0.20	0.50			11.9	3.95	0.02	0.011	2.24				0.022											0.0173
	9	0.007	0.20	0.50			11.5	3.53	0.01	0.012	1.56						0.012									0.0101
	10	0.019	0.21	0.51			12.1	4.07	0.02	0.011	1.93				0.043	0.015										0.0182
	11	0.008	0.19	0.49			11.8	4.79	0.03	0.016	3.95					0.020		0.035								0.0111
	12	0.027	0.21	1.49			11.6	0.99	0.02	0.026	0.38	0.58														0.0344
	13	0.012	0.19	1.51			11.9	0.98	0.02	0.053	1.14															0.0271
	14	0.011	0.20	1.53			9.2	1.20	0.03	0.012	0.90															0.0144
	15	0.012	0.19	1.50			13.1	0.75	0.02	0.011	0.37	0.45				0.025										0.0146
	16	0.011	0.22	1.48			12.1	0.01	0.02	0.013	0.91															0.0147
	17	0.019	0.19	1.51			11.9	1.66	0.02	0.055	1.43															0.0347
	18	0.010	0.22	1.49			10.6	1.39	0.02	0.013	1.22					0.014										0.0134
	19	0.015	0.23	1.49			11.7	1.10	0.03	0.011	0.37															0.0181
	20	0.019	0.19	1.56			11.1	0.89	0.02	0.012	0.11															0.0224
Tabl	1	0.014	0.22	0.45			12.3	4.26	0.02	0.024	0.89					0.010	0.062									0.0190
	2	0.010	0.25	0.47			12.3	3.86	0.02	0.047	1.01	0.24					0.094									0.0210
	3	0.010	0.23	0.42			12.2	2.25	0.02	0.025	0.96				0.047	0.016	0.052									0.0116
	4	0.006	0.24	0.43			13.2	4.21	0.02	0.026	2.16						0.066	0.016								0.0113
	5	0.013	0.25	0.44			12.2	5.16	0.02	0.015	1.81						0.054									0.0169
	6	0.011	0.23	0.49			12.6	2.42	0.02	0.023	0.89	0.51				0.038	0.042				0.031					0.0184
	7	0.009	0.24	0.42			12.6	4.55	0.02	0.031	1.60	0.24				0.042	0.05		0.002							0.0156
	8	0.015	0.23	0.46			12.7	3.56	0.02	0.011	0.84				0.022		0.1									0.0137
	9	0.008	0.23	0.48			12.3	3.75	0.02	0.012	1.44					0.023	0.074	0.012								0.0087
	10	0.011	0.25	0.53			12.7	4.51	0.02	0.011	1.52				0.043	0.043	0.066		0.005							0.0079
	11	0.010	0.23	0.49			11.8	5.59	0.02	0.016	2.63						0.119									0.0112
	12	0.008	0.21	0.53			11.9	0.76	0.02	0.066	0.38	0.58				0.057	0.047									0.0216
	13	0.012	0.24	0.44			11.9	2.65	0.02	0.053	1.14					0.007	0.064									0.0253
	14	0.011	0.25	0.43			9.5	2.61	0.02	0.012	0.06					0.006	0.009									0.0141
	15	0.012	0.22	0.50			12.2	3.28	0.02	0.011	0.37	0.45			0.025	0.035	0.026									0.0116
	16	0.011	0.22	0.49			12.3	0.81	0.02	0.013	0.41					0.004	0.01									0.0144
	17	0.019	0.27	0.51			12.1	4.62	0.01	0.066	1.43					0.020	0.066									0.0354
	18	0.020	0.22	0.50			10.3	3.42	0.02	0.013	1.22				0.014	0.018	0.12									0.0190
	19	0.015	0.21	0.57			11.8	1.38	0.03	0.011	0.37					0.076	0.066									0.0148
	20	0.019	0.20	0.52			12.4	0.96	0.02	0.012	0.11					0.007	0.044									0.0211

N:JP2002-105604A

	C	Si	Mn	P	S	Cr	Ni	Al	N	Mo	Cu	Co	W	Ti	Nb	V	Zr	Ca	Hf	Ta	Mg	REM	B	O	C-sol
A	0.012	0.31	1.35	0.02	0.001	12.6	5.12	0.02	0.014	1.86															0.0160
B	0.011	0.51	1.08	0.02	0.001	13.4	4.86	0.02	0.021	1.67					0.024	0.033									0.0166
C	0.009	0.31	1.26	0.02	0.001	11.6	3.19	0.02	0.014	1.99				0.047											0.0091
D	0.006	0.22	1.43	0.01	0.001	12.1	4.31	0.02	0.008	1.98						0.016	0.016			0.011					0.0095
E	0.010	0.21	1.04	0.02	0.002	12.2	4.59	0.01	0.012	1.86															0.0134
F	0.011	0.29	1.39	0.01	0.001	11.9	5.33	0.02	0.018	2.35															0.0161
G	0.010	0.25	1.53	0.01	0.001	12.8	4.55	0.02	0.008	1.78						0.027									0.0116
H	0.012	0.32	1.31	0.02	0.001	11.9	3.74	0.02	0.019	0.01															0.0174
I	0.011	0.33	1.38	0.02	0.002	9.9	4.29	0.02	0.023	2.06					0.011	0.047									0.0161
J	0.014	0.26	1.36	0.01	0.001	12.6	2.51	0.02	0.009	1.39				0.025											0.0145
K	0.031	0.31	1.38	0.02	0.002	12.1	3.92	0.02	0.012	1.59															0.0341
L	0.012	0.29	1.06	0.01	0.002	12.0	0.14	0.02	0.009	1.41															0.0146
M	0.009	0.30	1.19	0.01	0.001	12.3	4.36	0.02	0.075	1.66															0.0304
N	0.014	0.24	1.24	0.01	0.002	11.6	4.66	0.02	0.016	1.73				0.039											0.0163

Paper No.
05095

CORROSION2005

Effects of Thermal Cycle Conditions on Intergranular Stress Corrosion Cracking in Sweet Environment for Supermartensitic Stainless Steel

Yukio MIYATA and Mitsuo KIMURA
JFE Steel Corporation, Steel Research Laboratories
1-1, Kawasaki-cho, Handa, Aichi, 475-8611, Japan

Hanuo NAKAMICHI and Kaoru SATO
JFE Steel Corporation, Steel Research Laboratories
1-1, Minamiwatarida-cho, Kawasaki-ku, Kawasaki, Kanagawa, 210-0855, Japan

Noritsugu ITAKURA
JFE Steel Corporation, Chita Works
1-1, Kawasaki-cho, Handa, Aichi, 475-8611, Japan

Katsumi MASAMURA
JFE Steel Corporation, Tokyo Head Office
2-2-3, Uchisaiwai-sho, Chiyoda-ku, Tokyo, 100-0011, Japan

ABSTRACT

Intergranular stress corrosion cracking (IGSCC) in heat affected zone (HAZ) for supermartensitic stainless steel was studied. Two grades of the steel, lean and high grades, were heat-treated for simulating welding thermal cycles. Cracks were observed in some simulated HAZ specimens by all four methods of SCC test, U-bend, four point bent (4PB), slow strain rate technique (SSRT) and single edge notch bend (SENB) methods. It suggests that even smoothly machined specimen can detect IGSCC as long as the specimen is sensitized sufficiently and immersed in severe corrosion environment. Thermal cycle conditions inducing the cracking were clarified by U-bend SCC test for the lean and high grade steels. The results revealed that the high grade steel has higher resistance to IGSCC than the lean grade steel, and that post welding heat treatment (PWHT) is effective to prevent IGSCC. Chromium depleted zones were confirmed on prior austenite grain

Copyright
©2005 by NACE International. Requests for permission to publish this manuscript in any form, in part or in whole must be in writing to NACE International, Publications Division, 1440 South Creek Drive, Houston, Texas 77084-77084-4906. The material presented and the views expressed in this paper are solely those of the author(s) and not necessarily endorsed by the Association. Printed in U.S.A.

boundary adjacent to carbides that precipitated on the grain boundary for the lean grade steel. In these results, it was concluded that IGSCC in HAZ for supermartensitic stainless steel is caused by chromium depletion on prior austenite grain boundary accompanied by re-precipitation of chromium carbide during girth welding.

Keywords: supermartensitic stainless steel, intergranular stress corrosion cracking (IGSCC), sensitization, stress corrosion cracking (SCC), linepipe, girth welding

INTRODUCTION

Low carbon martensitic stainless steels, which are called supermartensitic stainless steels, have been developed for linepipes under sweet environments since the late 1990's [1]-[3]. They have contributed to oil and gas industry as alternative materials for duplex stainless steels or carbon steel with inhibitor [4]-[8].

However, new type of cracking of the steel has been reported on the basis of laboratory tests [9], [10]. The cracking occurs in the heat affected zone (HAZ) of girth welds and its morphology is intergranular stress corrosion cracking (IGSCC). Laboratory works show that post welding heat treatment (PWHT) is effective to prevent IGSCC and that cracks are observed only in root intact specimen on four point bent (4PB) SCC test, while no crack was observed in root machined specimen [9]. The most likely mechanism of the cracking was supposed to be sensitization, in other words, chromium depletion from the results of TEM analysis [10]. However, more precise analysis is required for a clear understanding of the mechanism. In-service failure caused by same type of cracking has also been reported [11]. Although the analysis suggested that welding conditions affect the cracking, they have not yet been proven quantitatively. Amaya et al. reported that the crack initiated the chromium depletion caused by surface oxidation during welding [12]. However, this cannot explain the propagation of the crack.

In this context, we studied effects of welding thermal cycle conditions on sensitization behavior by HAZ simulation. We also tried more precise analysis to investigate chromium distribution around grain boundary.

EXPERIMENTAL PROCEDURES

Materials

Two types of supermartensitic stainless steel pipe were investigated in this study. One was a lean grade supermartensitic stainless steel pipe, which contained 11% of Cr, 1.5% of Ni and no Mo. The other was a high grade one, which contained 12% of Cr, 5% of Ni and 2% of Mo. The chemical compositions are shown in Table 1. The pipe sizes for the lean and high grade steels were 273mm outer diameter with 12.7mm thickness and 355mm outer diameter with 12.6mm thickness, respectively.

HAZ simulation

The specimens were subjected to thermal cycles for HAZ simulation by Gleeble tester. They were smoothly machined and their dimension was 4mm thick and 15mm wide for U-bend and 4PB SCC tests or 11mm thick and 11mm wide for slow strain rate technique (SSRT) and single edge notch bent (SENB) SSC tests.

The thermal cycles basically consisted of one to three heat passes. The first pass was heated to 900 or 1300°C for 1 s. The conditions of the second pass were varied in the temperature of 450 to 750°C and the holding time of 1 to 10000 s. The third pass simulating PWHT was given to some specimens. The conditions of the third pass were varied in the temperature of 550 to 700°C and the holding time of 60 to 1000 s.

The rate of cooling on thermal cycle was adjusted by argon gas blow. Cooling time from 800 to 500°C was 9 s corresponding to 1.0 kJ/mm of heat input with 12.7 mm thickness plate.

SCC tests

In former studies, cracking occurred in only the specimen with root bead left intact, but never occurred in the smoothly machined specimen. Hence, more severe test was considered to be required in order to define the welding conditions inducing IGSCC with smoothly machined specimen. U-bend test method basically according to ASTM G30 was selected for this evaluation because more plastic strain could be induced to the specimen. In addition, more severe corrosion environment was also selected for the tests. The tests were carried out in 5% NaCl, pH 2.5 aqueous solution with 1 bar CO_2 at 70°C for the lean grade. And more severe conditions, pH 2.0 and 100°C, were selected for the high grade. The pH was adjusted by HCl addition. The test duration was 168 h.

After the conditions inducing sensitization were determined by U-bend test method, other test methods, 4PB, SSRT and SENB tests, were tried with the sensitized specimen. The 4PB tests were carried out in accordance with EFC 17. The specimens for the tests were prepared by polishing by abrasive paper in order to remove scales formed during heat treatment. Actual proof stress of base metal, 600 MPa for the lean grade and 620 MPa for the high grade steel, were applied to the specimens. Environmental conditions were as same as those in U-bend test. The specimens for SSRT and SENB tests were prepared by machining from sensitized specimens with 11mm and 11mm dimension. The SSRT tests were conducted at the strain rate of $8.0 \times 10^{-7} sec^{-1}$ in various environments. The sensitization was evaluated by the ratio of reduction area and elongation in corrosion environment to those in deionized water at same temperature. The other procedures were based on EFC 17. The SENB [13] tests were carried out at the target crack tip open displacement (CTOD) of 0.10 mm under the same environments as used in U-bend test. Average SCC length was determined by measurement of five positions of the length between crack tips of SCC and intentional fatigue notch.

The dimensions of these specimens for SCC tests are shown in Figure 1.

Micrographic investigations

Cross sectional observations of specimens after SCC tests were performed by optical microscope at 100-fold magnification to check any crack. SEM observations for cross section and fracture surface were also performed using a FE-SEM (LEO-1530).

TEM analysis for chromium distribution around grain boundary

Distribution of chromium concentration around grain boundary for sensitized lean grade steel was analyzed by TEM-EDX. Less than 100 μm thickness sheet of sample was prepared by cutting and mechanical polishing. Then, a TEM specimen was prepared by using a twin jet electrolytic polishing method. TEM analysis was carried out using a FE-TEM (Philips CM20-FEG) combined with an EDAX Phoenix system. The analyses were performed across the prior austenite grain boundary over about 100 nm in length with a 1.9 nm step. The acquisition time of each point was 15 s. A specimen drift compensation program was applied. The total drift was estimated to be less than 1 nm.

RESULTS AND DISCUSSION

Effects of thermal cycle conditions

Cracks were observed in some specimens of the lean and high grade steels with two pass thermal cycles after U-bend SSC tests. The cracks showed intergranular fracture surface as an example in Figure 2. It was therefore considered that U-bend test was reasonable method for evaluating IGSCC.

The test results for the lean and high grade steels are plotted as a function of temperature and holding time of the second pass as shown in Figure 3 and 4, respectively. The conditions of the first pass is 1300°C for 1 second. Micro crack means crack that could not detected visually but was detected by optical microscope at 100-fold magnification. For the lean grade steel, cracks were recognized in temperatures of 550 to 700°C and holding time of 1 to 25 s for the second pass. And cracks were also recognized in longer holding time at lower temperatures. No crack occurred in longer holding time at higher temperatures or shorter holding time at lower temperatures. For the high grade steel, cracks were recognized in lower temperatures and more limited conditions than the lean grade steel. However, behaviour of cracking for the high grade steel showed similar tendency to that for the lean grade steel.

Table 2 shows comparison of U-bend test results under various environmental conditions between the high and lean grade steels. No crack occurred in the high grade steels under the condition of pH 2.5 and 70°C, under which crack occurred in the lean grade. From these results, the high grade steel shows higher resistance to IGSCC.

No crack occurred in the specimen with only one pass thermal cycle of 1300°C for 1 second, without any following pass.

The effect of the first pass temperature was investigated by using the high grade steel. The temperature of the first pass was varied to 1300, 1100, 1000 and 900°C. The second pass condition was 450°C for 180 s, that induced to IGSCC in case of the first pass of 1300°C. While cracks were observed in the specimen with the first pass of 1300 and 1100°C, no crack was observed in those of 1000 and 900°C.

Effects of the third pass on the cracking behavior were tested. The specimens of the high grade steel were sensitized by the second pass of 450°C for 180 s followed by the third pass of various conditions simulating PWHT. The results are shown in Figure 5. No crack was observed in any specimen tested. From the results, PWHT of 550 to 700°C for 60 to 1000 s prevents IGSCC of the

high grade steel. It is noted that the optimum conditions of PWHT should be determined also on the basis of other properties such as hardness, resistance to sulfide stress cracking (SSC) and so on.

Mechanism of IGSCC

The results of SCC tests supported the hypothesis that IGSCC of these materials is caused by chromium depletion formed at grain boundary. Then, in order to prove the hypothesis, the sensitized specimen of the lean grade steel was investigated. The sensitized conditions were 1300°C for 1 s for the first pass and 650°C for 1 s for the second pass. Since investigations with an optical microscope did not reveal any clear carbide on the grain boundary of the sensitized specimen, SEM and TEM investigations were carried out.

Cross sectional view of the cracked lean grade specimen after U-bend test are shown in Figure 6. A crack propagates along prior austenite grain boundary and carbides precipitate along the grain boundary intermittently. TEM micrograph is shown in Figure 7. Prior austenite grain boundary with some carbides are observed. The carbides were identified as the type of $M_{23}C_6$ by EDX analysis. The analyzed chromium concentration on the basis of Cr and Fe binary quantification is also shown in Figure 7. Chromium depleted zones are clearly observed on the grain boundary adjacent to the carbides, shown in lines A and C. The minimum concentration of chromium is estimated to around 9 mass%. The width of the depleted zone is about 10 to 15 nm as half-value width. For the sensitized high grade specimen, SEM and TEM investigations have not so far revealed any clear carbide nor chromium depletion. Since the lean and high grade steel showed similar tendency of cracking behavior, the mechanism was supposed to be same in the two grades of steel. Further investigation is required for a clear understanding of the mechanism for the high grade steel.

The results of the SCC test support that this phenomenon is caused by chromium depletion accompanied by carbide precipitation during girth welding. Diffusion of chromium would explain the recovery from the sensitization by additional heat input. Figure 8 shows the average diffusion length of chromium in alpha-ferrite. The results of SCC tests for the lean grade steel are also plotted in the graph. The graph shows the lean grade steel would be sensitized under the conditions of the heat input corresponding to the chromium diffusion length of 1 to 20 nm. In other words, chromium depleted zone would be healed if sufficient heat input corresponding to the length of 20 nm was applied.

From these results and consideration, change in carbide and chromium distribution around prior austenite grain boundary is proposed as follows.

1) Before welding, carbides are present in both matrix and grain boundary owing to the heat treatment at pipe production. Distribution of chromium across grain boundary is homogenized.
2) After high temperature heat pass, which is higher than Ac_3 point, carbides decompose and carbon is dissolved into austenite matrix. Chromium distribution is also homogenized in this stage.
3) In case that the following pass with some specific conditions after high temperature heat pass is applied, carbides re-precipitate along prior austenite grain boundary intermittently. Chromium depleted zone is formed on the grain boundary adjacent to the carbides.
4) Even though once sensitized, in case that appropriate consequent pass is applied, the depleted zone is healed due to chromium diffusion from matrix.
5) Therefore, sensitization requires at least two welding passes, the pass for dissolution of carbon followed by the pass for precipitation of carbide.

Test method for IGSCC

The thermal cycle conditions inducing sensitization were confirmed by the U-bend SCC tests. Then, various test methods were tried by using sensitized specimens. The thermal cycle conditions for sensitization were 1300°C for 1 s and 650°C for 1 s for the lean grade and 1300°C for 1 s and 450°C for 180 s for the high grade steel.

The experimental conditions and results of the 4PB tests are summarized in Table 4. All specimens for the tests had machined smooth surface. Crack was observed in the sensitized specimen after 168 h immersion. It was proved that IGSCC can be detected by 4PB test using machined surface specimen as long as specimen is sensitized sufficiently and immersed in severe environmental conditions. Although dimension of specimen would be one of the factors, which affect on cracking behavior, root intact specimen would not be a necessary condition for IGSCC.

The experimental conditions and results of the SSRT tests are summarized in Table 5. And stress-strain curves for the lean grade steel are shown in Figure 9. Lower elongation is observed in the conditions of lower pH or higher NaCl concentration than in those of higher pH or lower NaCl concentration. Degree of sensitization can be evaluated quantitatively by SSRT test.

The experimental conditions and results of the SENB tests are summarized in Table 6. The values of actual CTOD were little bit smaller than that of target one. SCC was recognized in the lean grade steel, while no SCC in the high grade steel. The average SCC length for the lean grade steel was 2.7mm.

From these results, it was concluded that even smoothly machined specimen can detect IGSCC by all four test methods, U-bend, 4PB, SSRT and SENB tests as long as the specimen is sufficiently sensitized and immersed in a severe corrosion environment.

CONCLUSIONS

Intergranular stress corrosion cracking (IGSCC) in heat affected zone (HAZ) was studied by using two grades, lean and high, of supermartensitic stainless steel subjected to simulated welding thermal cycle. Conclusions are summarized as follows:

1) IGSCC in HAZ for supermartensitic stainless steel is caused by chromium depletion, in other word sensitization, on prior austenite grain boundary accompanied by re-precipitation of chromium carbide during girth welding.
2) Chromium depleted zones were recognized in the lean grade steel specimen with two-pass thermal cycle. They were on prior austenite grain boundary adjacent to carbide that precipitate on the grain boundary. The minimum concentration of chromium was estimated to around 9 mass%. The width of the depleted zone was about 10 to 15 nm as half-value width.
3) The sensitization requires at least two welding passes, the pass for dissolution of carbon followed by the pass for precipitation of carbide.
4) All four test methods, U-bend, four point bent (4PB), slow strain rate technique (SSRT) and single edge notch bend (SENB) SCC tests, can detect IGSCC as long as specimen is sufficiently sensitized and immersed in a severe corrosion environment.
5) Thermal cycle conditions inducing the cracking were clarified by U-bend SCC test for the lean and high grade steels.

6) The high grade steel has higher resistance to IGSCC than the lean grade steel. The cracking for the high grade steel occurs in smaller range of thermal cycle conditions under more severe environmental conditions than for the lean grade steel.
7) Application of post welding heat treatment (PWHT) is effective to prevent IGSCC for the lean and high grade steel.

REFERENCES

1. M. Ueda, H. Amaya, K. Kondo, K. Ogawa and T. Mori, Corrosion 96, Paper No.58, (1996).
2. Y. Miyata, M. Kimura and F. Murase, Kawasaki Steel Technical Report, 38(1998) 53.
3. K. Nose, H. Asahi, H. Tamehiro and H. Inoue, Proceedings of the 16th International Conference on OMAE, 3(1997) 107.
4. T. Barnett, Eurocorr98, (1998).
5. S. A. Duthie, Offshore Technology Conference, OTC8716, (1998).
6. K. van Thoor, Stainless Steel World November 1999, (1999) 42.
7. P. E. Kvaale and S. Olsen, Stainless Steel World 99 Conference, SSW99-202, (1999) 19.
8. E. Warren and J.Bowers, Stainless Steel World March 2003, (2003) 50.
9. T. Rogne and M. Svenning, Supermartensitic Stainless Steels 2002, No.P024 (2002).
10. E. Ladanova, J. K. Solberg and T. Rogne, Supermartensitic Stainless Steels 2002, No.P028 (2002).
11. Gregori, P. Woollin and W. van Gestel, Stainless Steel World December 2003, (2003) 17.
12. H. Amaya, K. Kondo, A. Taniyama, M. Sagara, K. Ogawa, T. Murase, H. Hirata, H. Takabe and M. Ueda, Corrosion2004, Paper No.04124, (2004)
13. T. Rogne, B. Nyhus, M. Svenning, H. I. Lange, O. Ørjasæter and T. G. Eggen, Corrosion2003, Paper No.03534, (2003)

TABLE 1
CHEMICAL COMPOSITIONS OF STEEL USED

(mass%)

Material	C	Si	Mn	Cr	Ni	Cu	Mo	N
Lean grade	0.013	0.16	1.13	11.1	1.5	0.5	-	0.011
High grade	0.007	0.14	0.64	12.1	5.7	-	2.1	0.007

TABLE 2
EFFECTS OF ENVIRONMENTAL CONDITIONS ON SCC BEHAVIOR

Material	Conditions of the 2nd. pass	pH 2.5 70°C	pH 2.5 100°C	pH 2.0 100°C
Lean grade	650°C for 1s	Crack	-	Crack
High grade	500°C for 50s	No crack	No crack	Crack

Conditions of the first pass: 1300°C for 1s
Test method: U-bend test
Other environmental conditions: 5% NaCl, 1bar CO_2, 168 h

TABLE 3
EFFECTS OF THE FIRST PASS TEMPERATURE ON SCC BEHAVIOR

Material	Conditions of the 1st. pass	Conditions of the 2nd. pass	SCC test result
High grade	1300°C for 1s	450°C for 180 s	Crack
	1100°C for 1s		Crack
	1000°C for 1s		No crack
	900°C for 1s		No crack

Test method: U-bend test
Environmental conditions: 5% NaCl, pH2.0, 1bar CO_2, 100°C, 168 h

TABLE 4
RESULTS OF 4PB SCC TESTS FOR SIMLATED HAZ

Material	NaCl (%)	pH	CO_2 (bar)	Temp (°C)	Applied stress (MPa)	Duration (h)	Result
Lean grade	5.0	2.5	1.0	70	600	168	Crack
High grade	5.0	2.0	1.0	100	620	168	Crack

TABLE 5
RESULTS OF SSRT SCC TESTS FOR SIMULATED HAZ

Material	Test conditions					Test results	
	NaCl (%)	pH	CO_2 (bar)	Temp (°C)	Strain rate (/s)	El ratio (%)	RA ratio (%)
Lean grade	5.0	2.5	1.0	70	$8.0x10^{-7}$	64.8	38.7
	5.0	4.5	1.0	70	$8.0x10^{-7}$	66.7	35.0
	1.0	4.5	1.0	70	$8.0x10^{-7}$	78.4	47.1
	0.2	4.5	1.0	70	$8.0x10^{-7}$	95.7	97.9
	Deionized water		-	70	$8.0x10^{-7}$	100.0	100.0
High grade	5.0	2.0	1.0	100	$8.0x10^{-7}$	59.3	31.0
	5.0	2.5	1.0	70	$8.0x10^{-7}$	96.3	88.7
	Deionized water		-	70	$8.0x10^{-7}$	100.0	100.0

TABLE 6
RESULTS OF SENB SCC TESTS OF SIMULATED HAZ

Material	NaCl (%)	pH	CO2 (bar)	Temp (°C)	Duration (h)	Target CTOD (mm)	Actual CTOD (mm)	SCC length (mm)	Comment
Lean grade	5.0	2.5	1.0	70	168	0.10	0.082	2.7	SCC
						0.10	0.094	2.7	SCC
High grade	5.0	2.0	1.0	100	168	0.10	0.087	0.0	No SCC
						0.10	0.096	0.0	No SCC

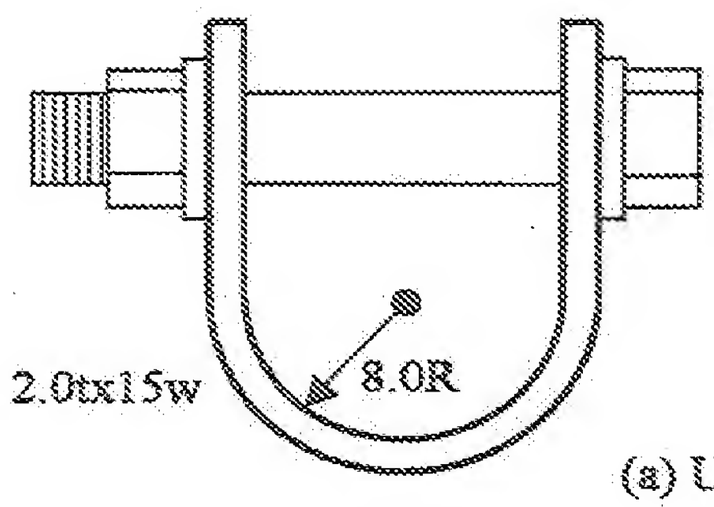

(a) U-bend specimen

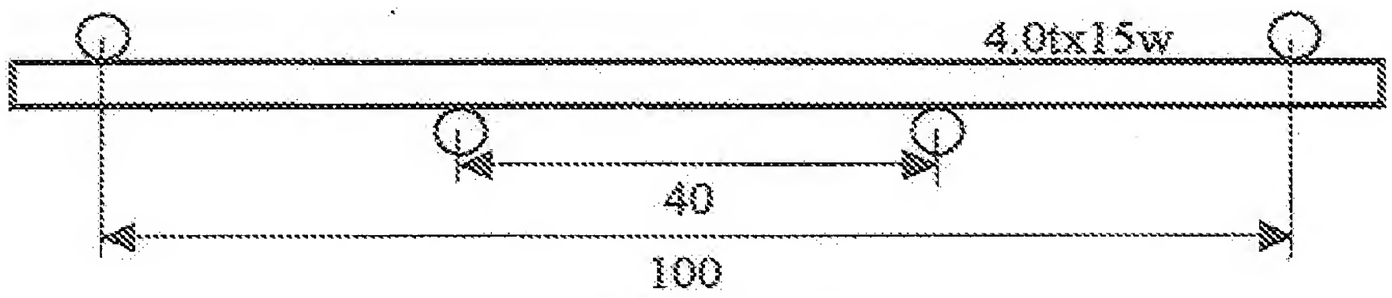

(b) 4PB specimen

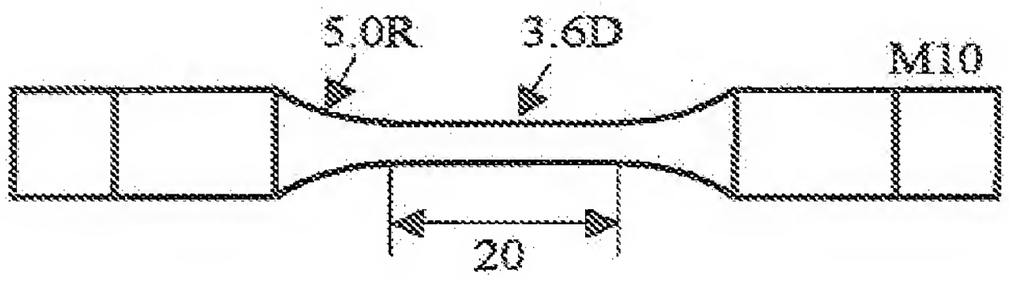

(c) SSRT specimen

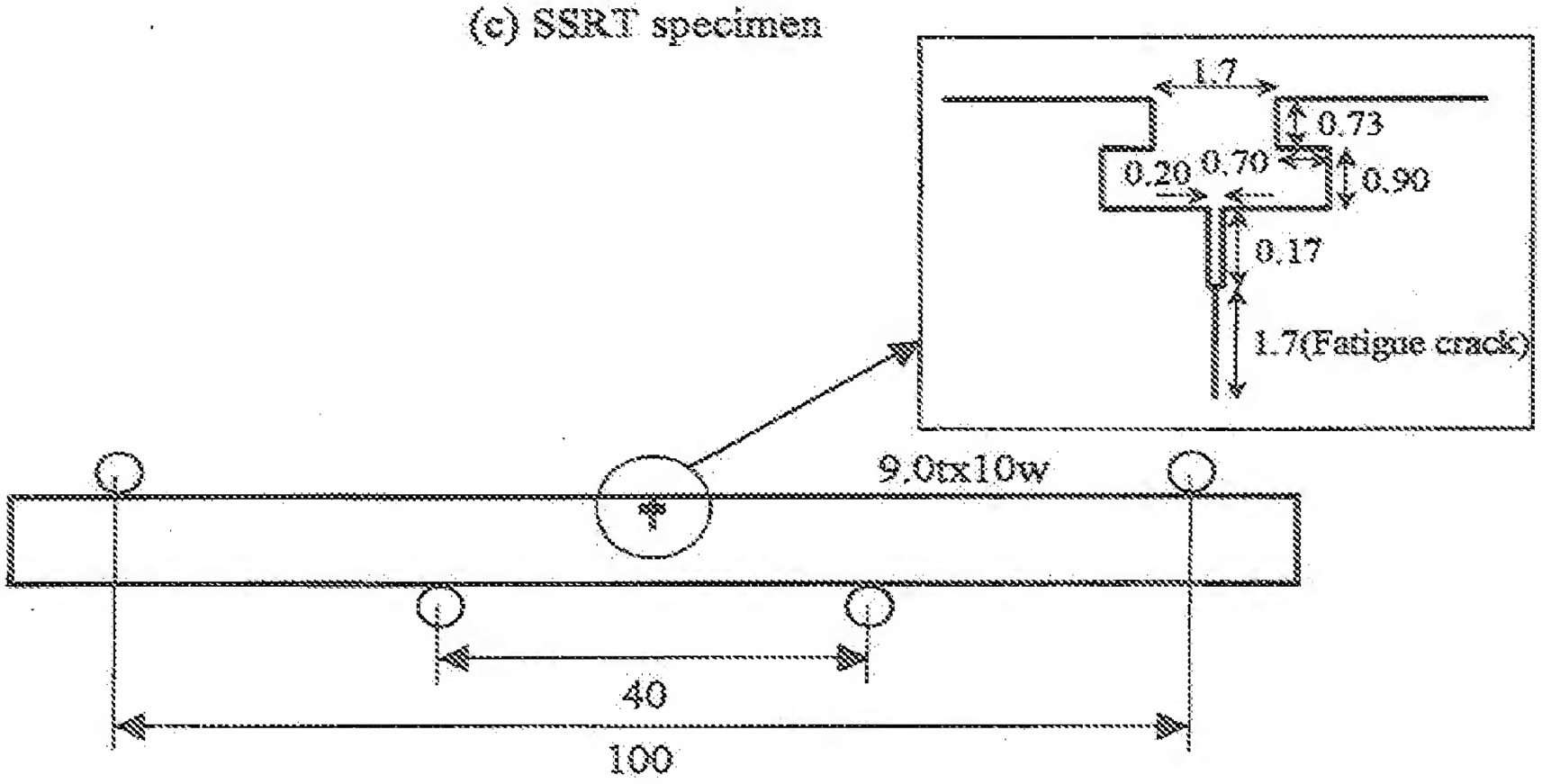

(d) SENB specimen

FIGURE 1 - Schematic illustration of specimens for SCC tests

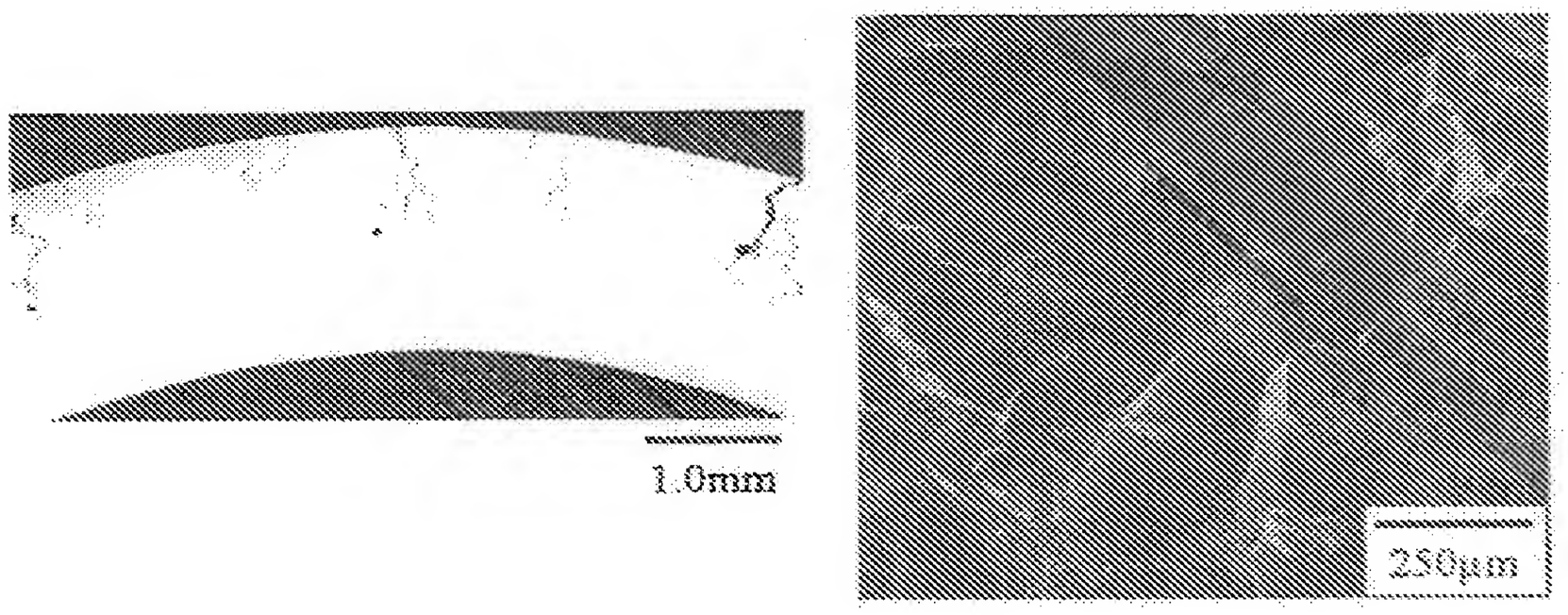

FIGURE - 2 Cross sectional view and fracture surface of the lean grade steel after SCC test (Thermal cycle conditions: 1300°C for 1s and 650°C for 1s)

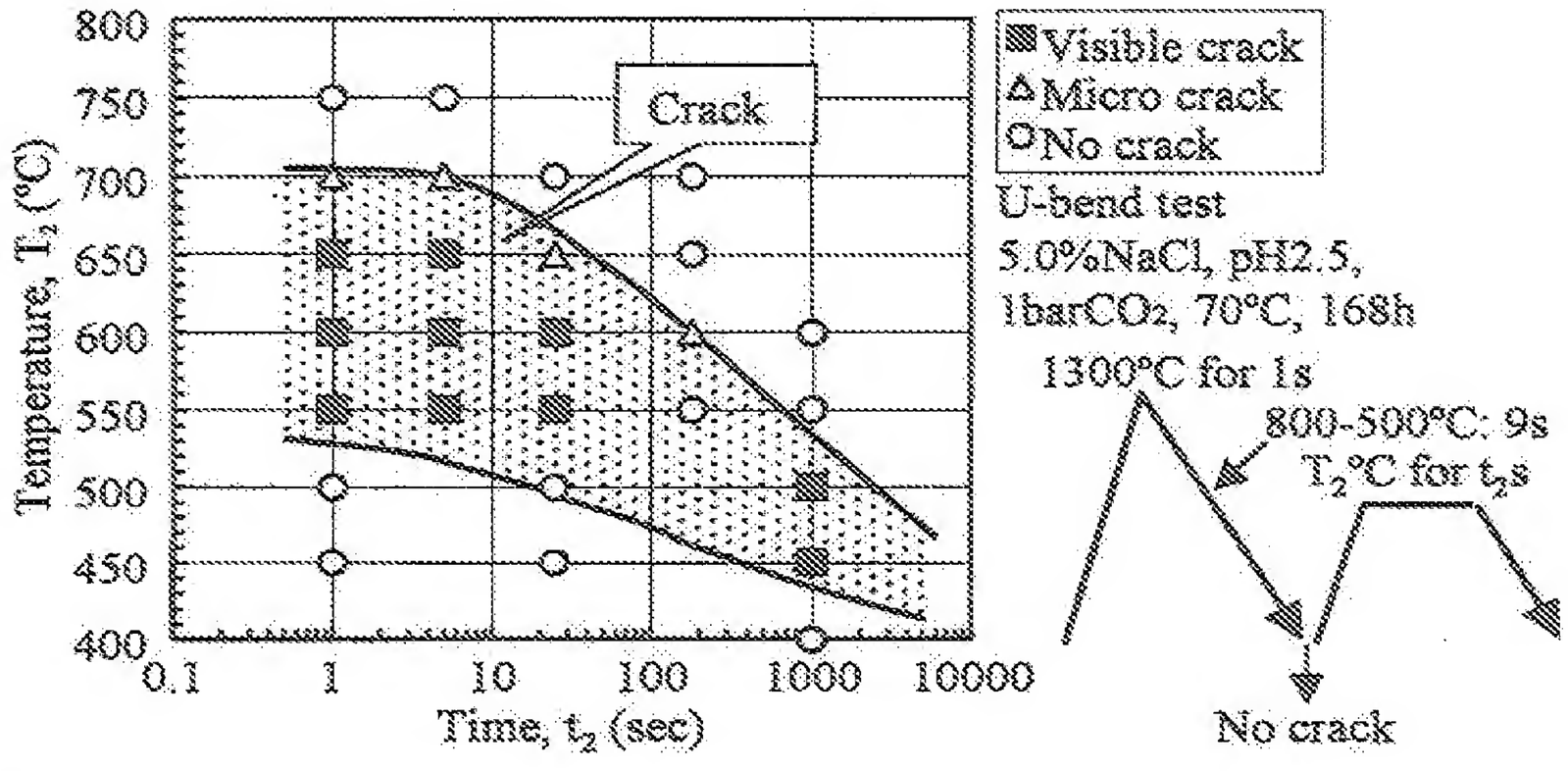

FIGURE - 3 Results of U-bend SCC tests for simulated HAZ of the lean grade steel

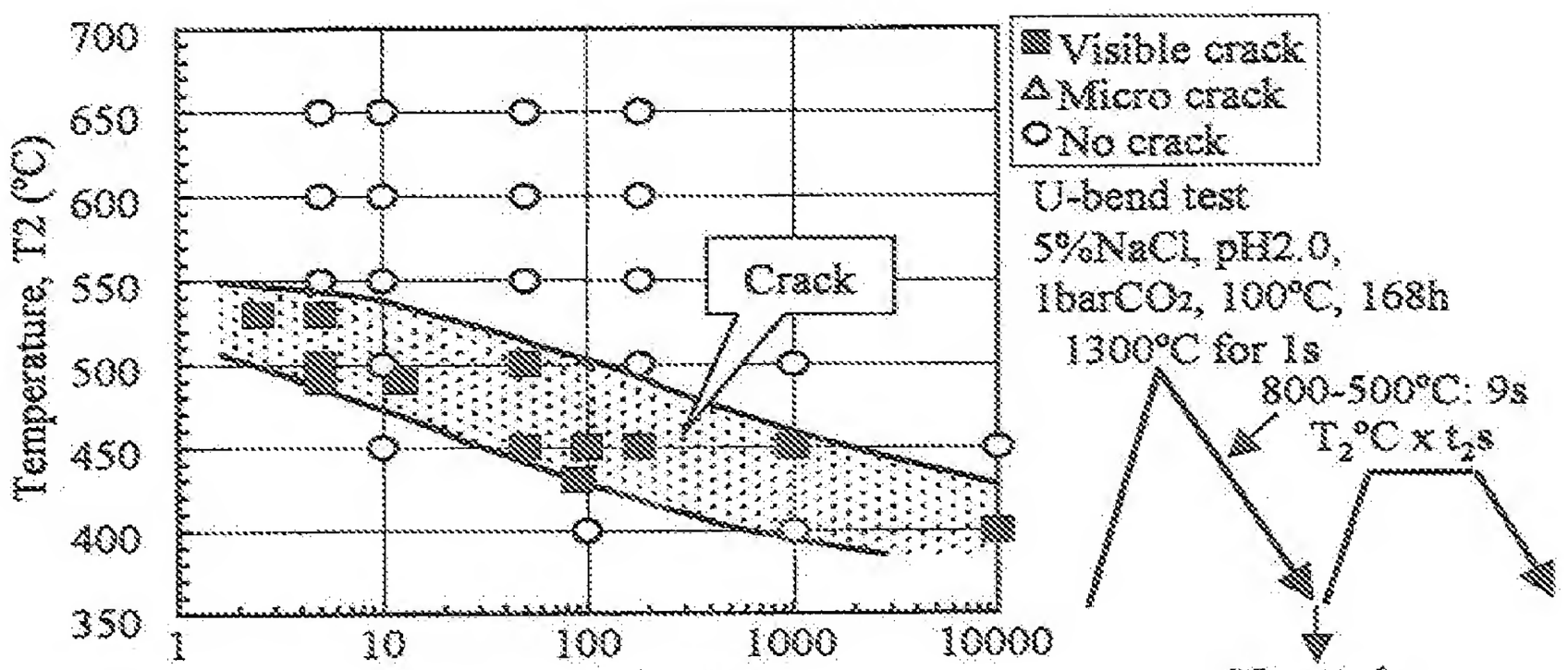

FIGURE – 4 Results of U-bend SCC tests for simulated HAZ of the high grade steel

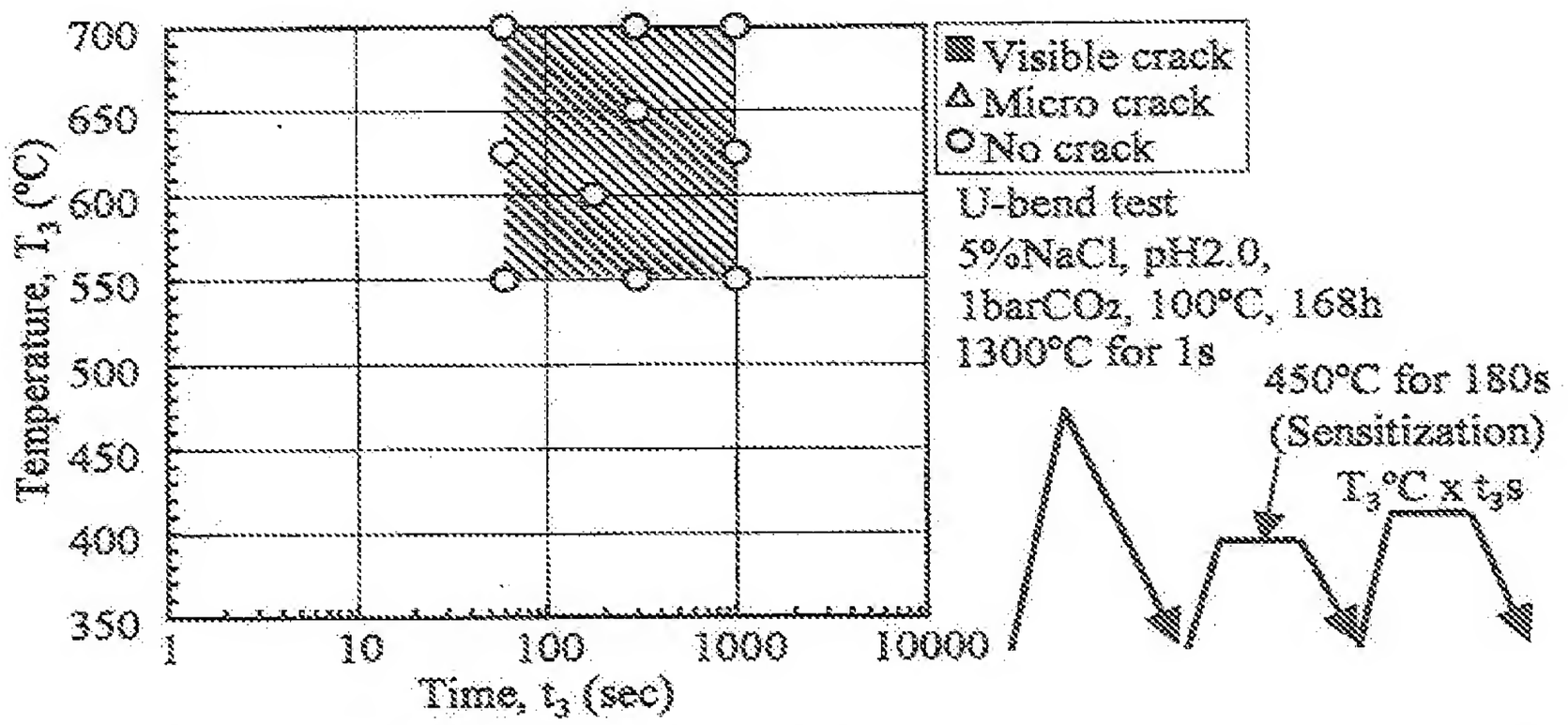

FIGURE - 5 Effects of thermal cycle conditions after sensitization on SCC behavior for the high grade steel

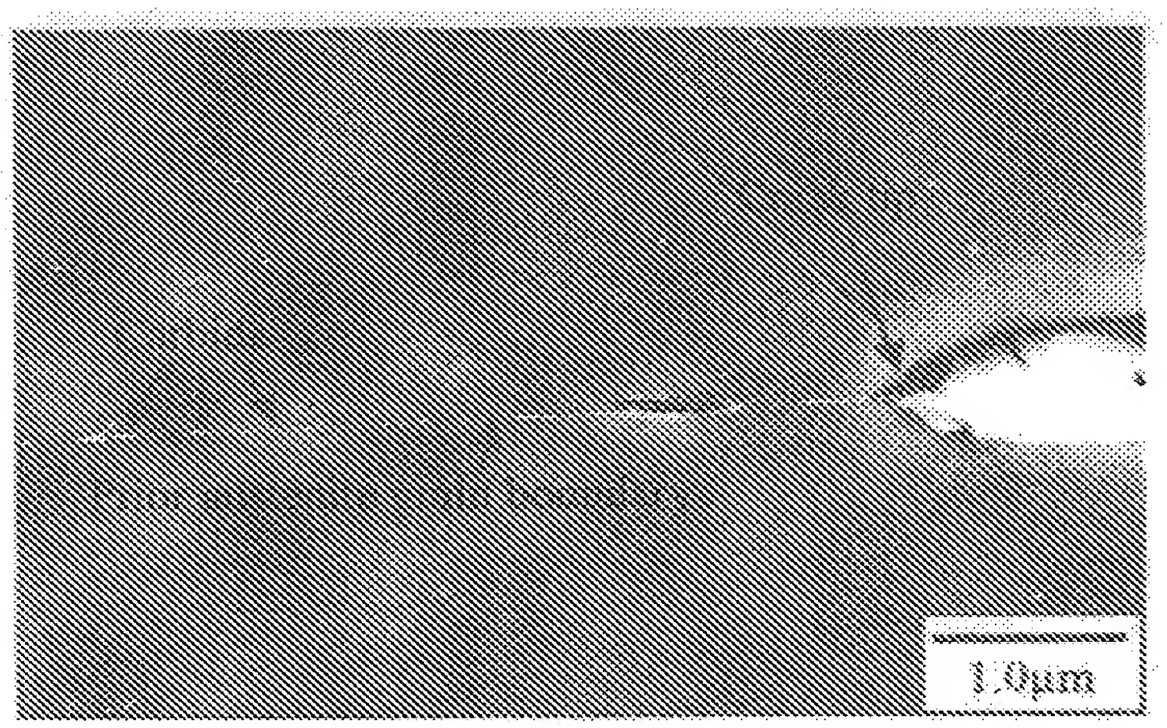

FIGURE - 6 Cross sectional view of crack tip area for the lean grade steel after SCC test (Thermal cycle conditions: 1300°C for 1s and 650°C for 1s)

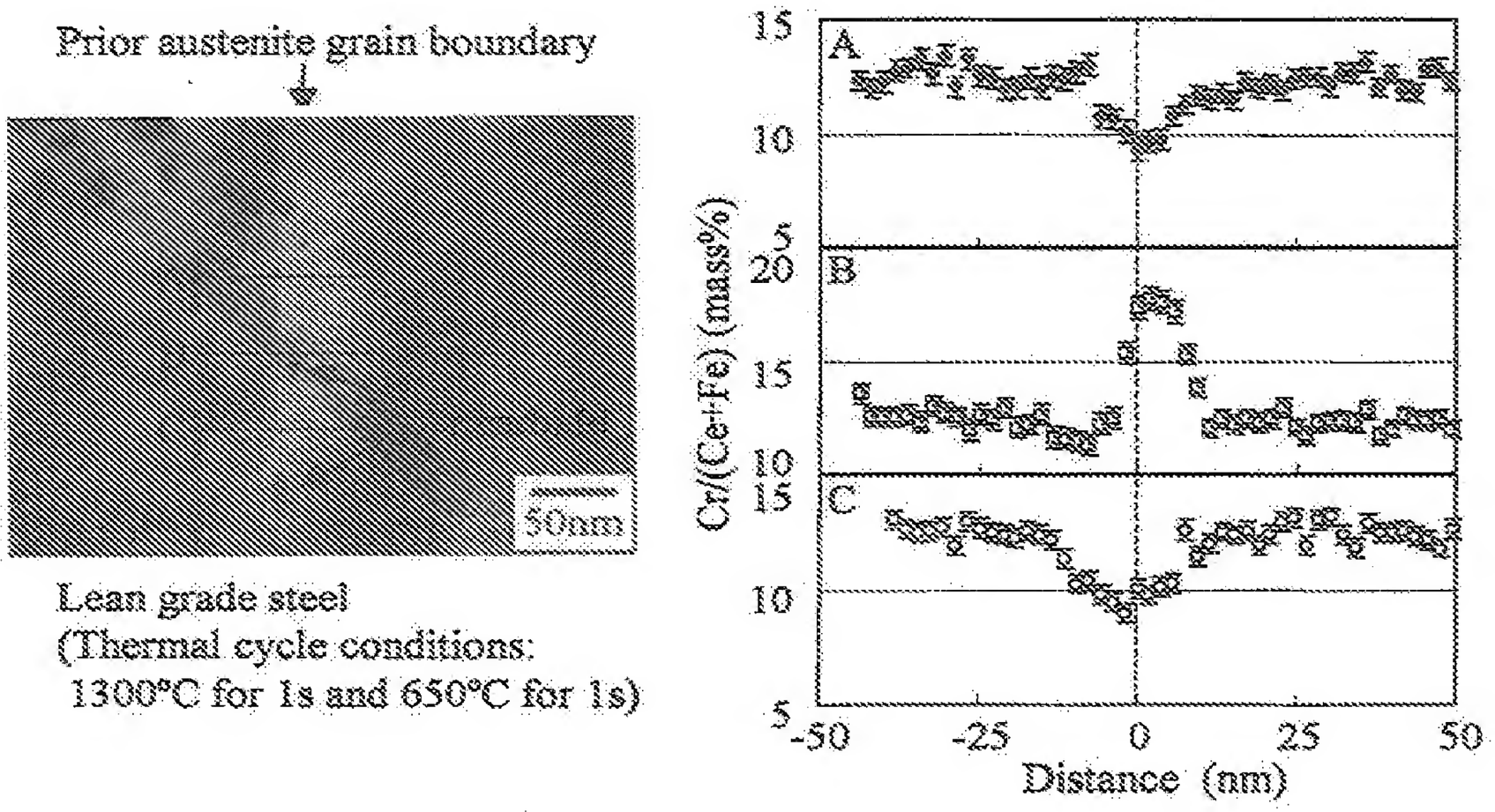

FIGURE - 7 Distributions of Cr concentration at the prior austenite grain boundary of the sensitized lean grade steels, analyzed by TEM-EDX

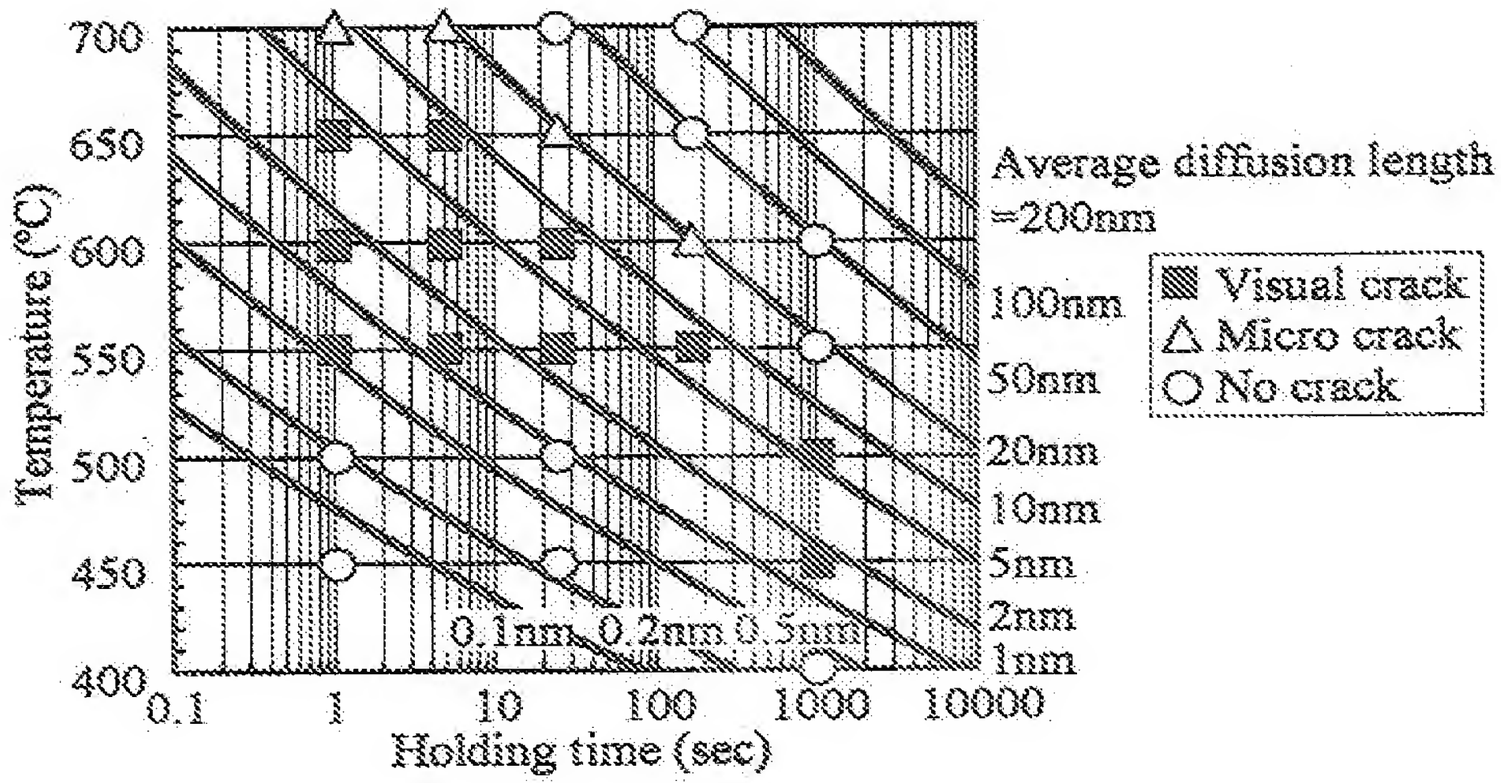

FIGURE - 8 Estimated results of average diffusion length of Cr in alpha-ferrite and correspondence of crack occurrence for the lean grade steel

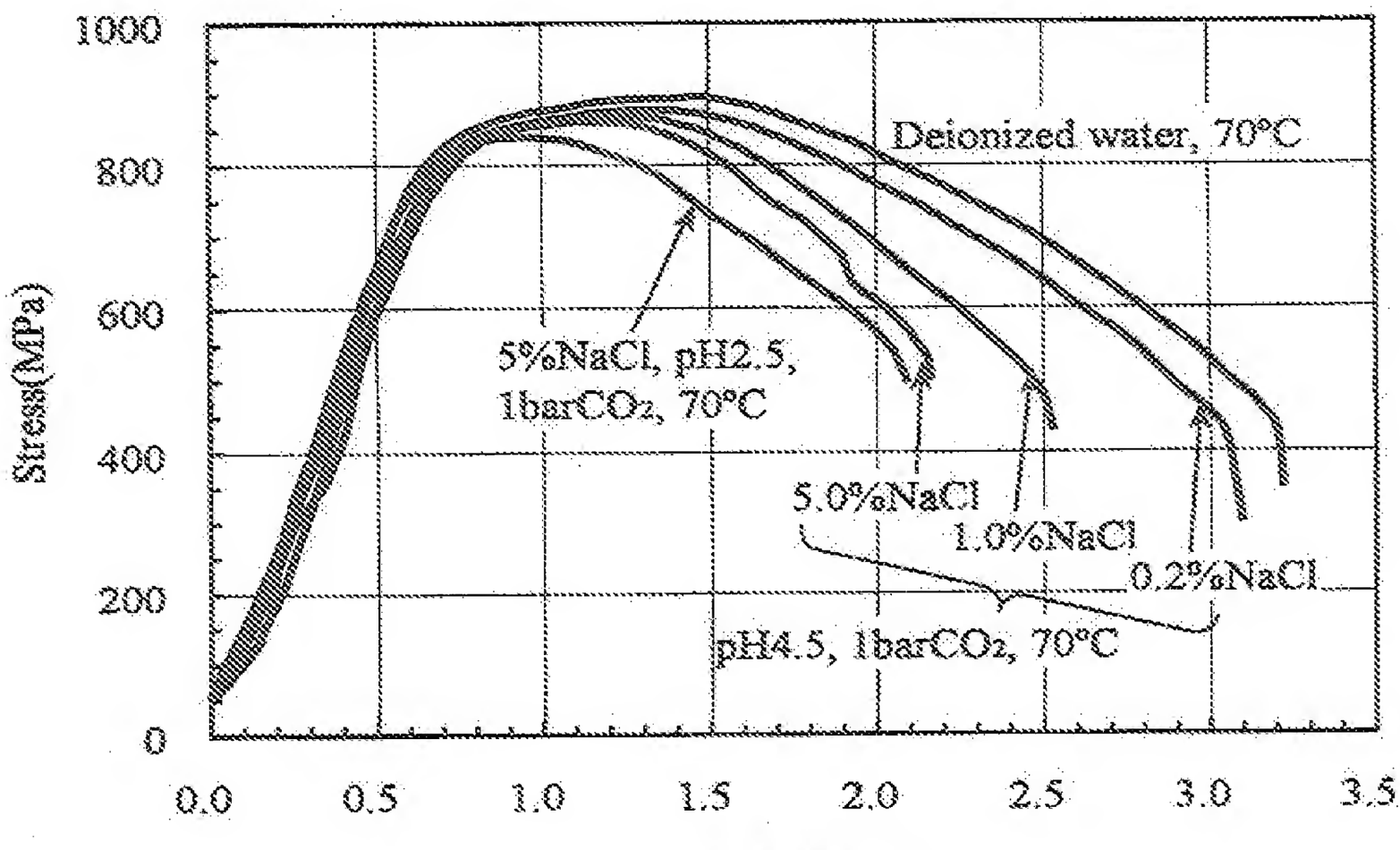

FIGURE - 9 Change in stress with strain during SSRT test for the lean grade steel

JFE TECHNICAL REPORT
No. 7 (Jan. 2006)

Martensitic Stainless Steel Seamless Pipe for Linepipe†

MIYATA Yukio*1 KIMURA Mitsuo*2 KOSEKI Tomoya*3

Abstract:

A martensitic stainless steel seamless pipe for linepipe application, KL-HP12CR, has been developed with good weldability, mechanical properties and corrosion resistance. Weldability is improved by the reduction of both C and N content. C reduction is also effective to the improvement of CO_2 corrosion resistance achieving the corrosion rate less than 0.127 mm/y under the CO_2 environment at 160°C and 2.0 MPa. It can be applied under the H_2S environment at pH4.0 and 0.001 MPa, since the resistance to sulfide stress cracking (SSC) is improved by Mo addition. The pipe has X80-grade strength and sufficient low temperature toughness for the practical use as a linepipe. Post weld heat treatment (PWHT) in a few minutes, the reduction of C content and addition of Ti are effective to prevent intergranular stress corrosion cracking (IGSCC) at the heat affected zone. Further application of the pipe is expected for the transportation of product fluid with corrosive gas such as CO_2, as an economical material with low life cycle cost.

1. Introduction

Due to increasing concern about the depletion of oil resources, oil and gas wells are being operated at ever-higher temperatures and pressures, and the production fluid generally contains CO_2, making it more corrosive. As a result, it is important to prevent CO_2 corrosion for the pipelines called flowlines and gatheringlines which transport the fluid before eliminating corrosive substances and water. Furthermore, the fluid often contains trace amounts of H_2S, so measures to prevent sulfide stress cracking (SSC) are also needed. Under such corrosive environments, the conventional method of preventing corrosion is to use carbon steels as the linepipe material and to inject an inhibitor into the fluid[1]. Corrosion prevention by an inhibitor, however, increases the operating cost particularly in offshore pipelines, so inhibitors are being used less, particularly in view of the recent focus on life cycle cost. Another reason for not using inhibitors is concern about pollution caused by accidental leakage. Therefore, there is demand for an economical material for linepipes that does not require an inhibitor. Existing corrosion resistant alloys for linepipes include duplex stainless steels[2,3], but these have drawbacks of very high material cost, difficulty in controlling the welding heat input, and excess anticorrosion action in many cases, even though the steels have excellent corrosion resistance.

In comparison, martensitic stainless steels generally show poor weldability, and require preheating and long post welding heat treatment (PWHT). Consequently, martensitic stainless steels are rarely used for pipelines in view of pipe-laying efficiency. Nevertheless, martensitic stainless steels have an appropriate level of CO_2 corrosion resistance, and are inexpensive compared with duplex stainless steels.

With this background, JFE Steel has used its extensive steel-making technologies to improve the weldability of martensitic stainless steels by decreasing the C and N contents, and by controlling the added alloying elements, thus developing a martensitic stainless steel seamless pipe for linepipes offering excellent weldability and corrosion resistance. This paper describes the development and characteristics of the steel pipe.

---

† Originally published in *JFE GIHO* No. 9 (Aug 2005), p. 13–18

*1 Senior Researcher Manager,
Tubular Products & Casting Res. Dept.,
Steel Res. Lab.,
JFE Steel

*2 Dr. Eng.,
Senior Researcher Deputy General Manager,
Tubular Products & Casting Res. Dept.,
Steel Res. Lab.,
JFE Steel

*3 Staff Deputy General Manager,
Products Service & Development Sec.,
Products Service & Development Dept.,
Chita Works,
JFE Steel

Table 1 Results of y-groove cracking tests for low C + N martensitic stainless steels

Material		Preheating temperature		
		30°C	70°C	100°C
0.03C-0.01N	11Cr-1.0Ni-0.5Cu	Crack	Crack	Crack
0.01C-0.03N		Crack	Crack	Crack
0.01C-0.01N	12Cr-1.0Ni-0.5Cu	No crack	No crack	No crack
	12Cr-1.0Ni-1.0Cu	No crack	No crack	No crack
	12Cr-2.0Ni-0.5Cu	No crack	No crack	No crack

Plate thickness: 15 mm
Welding material: Type 410M SMAW, 4φ (Diffusible hydrogen; 4.28 cm³/100 g)
Welding conditions: Current; 160 A, Voltage; 24–26 V, Speed; 150 mm/min
Test conditions: Room temperature; 30°C, Humidity; 60%RH

2. Progress of Development

2.1 Target Characteristics

The target characteristics for development were as listed below.

(1) Weldability: Welding without preheating
(2) HAZ maximum hardness: HV330 or smaller
(3) CO_2 corrosion resistance: Resistance to a corrosive environment of 5% NaCl, CO_2 partial pressure of 3.0 MPa, 150°C
(4) SSC resistance: Resistance to an environment of 5% NaCl, 0.001 MPa H_2S, pH4.0
(5) Strength: X80 grade (550 MPa or higher yield strength (YS))
(6) Low temperature toughness: 100 J or larger Charpy absorbed energy at −40°C

2.2 Composition Design Concept

The composition of the steel pipe was designed considering the effects of alloying elements in the martensitic stainless steel on the weldability, corrosion resistance, hot-workability, and other characteristics. Specifically, the improvement of weldability was studied based on a composition of KO-13Cr (0.20C-13Cr-0.03N) for OCTG for a CO_2 environment, while maintaining equivalent corrosion resistance in the base material. From the results of the study concerning the effect of chemical composition on the hot-workability and other characteristics mentioned below, the composition of the steel was ultimately determined to be 12Cr-5Ni-2Mo-0.01N with 0.015% or less C.

2.2.1 Weldability

Since welding of martensitic stainless steels tends to cause weld cracking, preheating is applied to prevent cracking in practice. Weld cracking is thought to be caused by hydrogen which is dissolved in the weld metal and the heat affected zone (HAZ) of the weld, and by the hardening and residual stress induced by the martensitic transformation at the HAZ[3]. Accordingly, an effective means to prevent weld cracking, from the material side, is to decrease the C and N contents and hence suppress the hardening induced by the martensitic transformation. Table 1 shows the result of the y-groove weld cracking test on low C + N martensitic stainless steels[4]. Steels containing 0.03% of C or N suffered weld cracking, while steels in which both the C and N contents were reduced to 0.01% did not suffer weld cracking even at the preheating temperature of 30°C. This result suggests that welding without preheating is possible only if the C and N contents are decreased to 0.01%. JFE Steel has the steel making technology to produce steels with such low C and N level.

2.2.2 CO_2 corrosion resistance

Reduction in the C content also improves the CO_2 corrosion resistance. Figure 1 shows the result of CO_2 corrosion tests for martensitic stainless steels having various chemical compositions[4]. The corrosion rates given in the figure show good correlation with the CO_2 corrosion indexes defined by Cr − 19C + 2Ni. The figure shows that increasing the Cr or Ni content and decreasing the C content improve the CO_2 corrosion resistance. This improvement is presumably because the reduction in the C content decreases the amount of Cr carbide, thereby increasing the amount of dissolved Cr which effectively prevents corrosion.

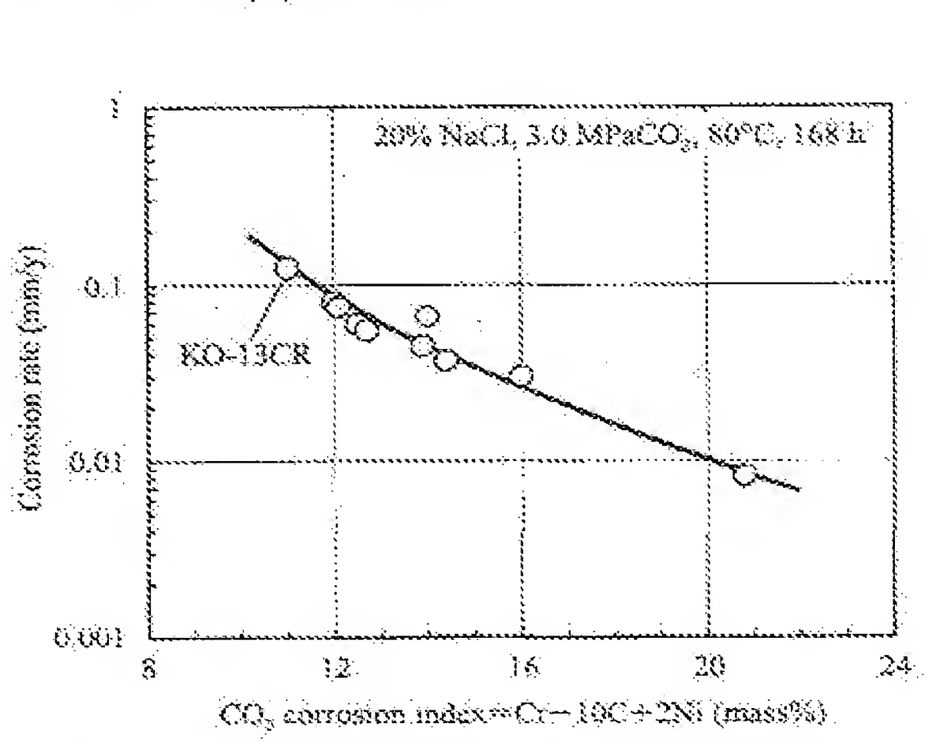

Fig. 1 Relationship between corrosion rate and CO_2 corrosion index

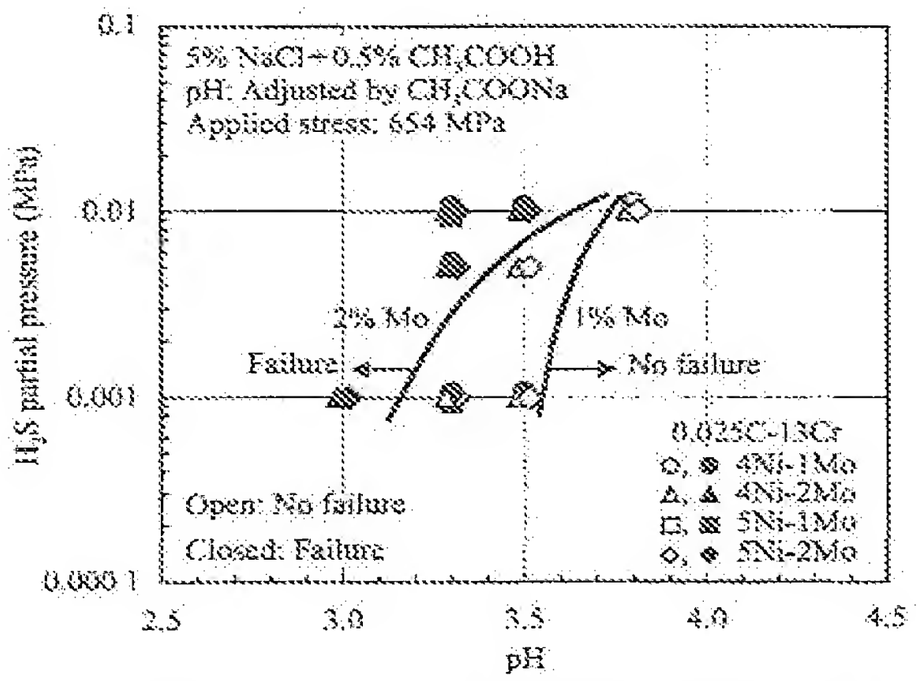

Fig. 2 Effects of Ni and Mo on SSC resistance of 0.025C-13Cr steels

2.2.3 SSC resistance

Since SSC in martensitic stainless steels begins from pitting, improving the resistance to pitting improves the SSC resistance. The alloying element molybdenum is known to improve resistance to pitting. **Figure 2** shows the effects of Ni and Mo on the SSC resistance[5]. As can be seen, an increase in the Ni content from 4% to 5% makes no difference to the test results, while increasing the Mo content from 1% to 2% moves the boundary of SSC occurrence toward low pH and high H_2S partial pressure, or to severer environments. This phenomenon suggests that adding 1% Mo is sufficient to ensure SSC resistance under the environment of 5% NaCl, 0.001 MPa H_2S, pH4.0, which is the development target. Since, however, the resistance to pitting at the HAZ may become lower than that of the base material[6], 2% Mo was added to the developed material to secure stable resistance to pitting.

Table 2 Chemical compositions of base metal and welding wires for girth welding

(mass%)

Material	C	Cr	Ni	Mo	N
Base metal	<0.015	13.0	5.3	2.0	0.01
GTAW wire	0.01	25.3	9.5	4.0	0.27
GMAW wire	0.02	25.1	9.6	4.0	0.27

3. Characteristics of Developed Steel Pipe

This capter describes the characteristics of the developed steel, focusing on the results of tests on a seamless steel pipe of 273 mm in outer diameter and 12.7 mm in wall thickness. A seamless steel pipe was manufactured with the steel having the chemical composition shown in **Table 2**, which was then treated by quenching and tempering to obtain an X80 grade product. With this product, and using 25Cr duplex stainless steel as welding material, a girth welded joint was prepared by applying GTAW to the first pass, and GMAW to the second pass. The chemical compositions of the respective welding materials are given in Table 2, and the welding conditions are given in **Table 3**. No preheating or PWHT was given.

3.1 Mechanical Properties

Table 4 shows the results of tensile tests. The strength of X80 grade was assured, and the welded joint fractured in the base metal, thus showing favorable characteristics. **Figure 3** shows the hardness distribution of a cross section of the welded joint. As shown, the

Table 4 Result of tensile tests for the welded joint and base metal

Material	YS (MPa)	TS (MPa)	El (%)	Fracture position
Welded joint	–	856	30	Base metal
Base metal	634	827	34	–

YS: Yield strength, TS: Tensile strength, El: Elongation

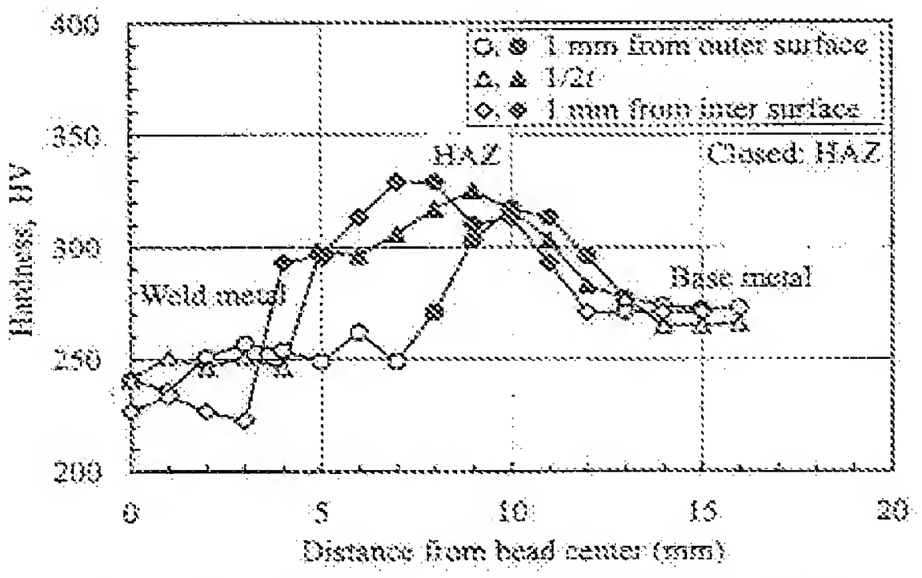

Fig. 3 Hardness distribution in the welding joint

Table 3 Girth welding conditions

Pass	Welding method	Welding material	Welding position	Shielding gas	Interpass temperature (°C)	Current (A)	Voltage (V)	Speed (mm/min)	Heat input (kJ/mm)
1	GTAW	2.0 mmφ	5G	100% Ar	<25	148	13.5	44	2.9
2	GMAW	1.2 mmφ	5G	100% Ar	25	145	15.0	75	1.7

5G: Horizontal fixed position

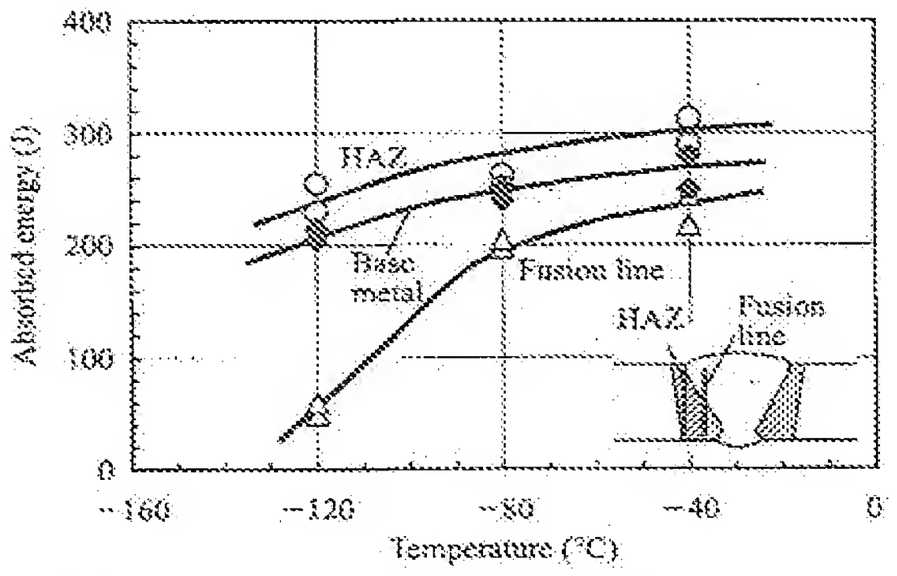

Fig.4 Relationship between Charpy absorbed energy and temperature

maximum hardness at the HAZ is about HV330, which satisfies the target value of HV350 or smaller. **Figure 4** shows the result of Charpy tests for the welded joint. The attained absorbed energy is about 200 J even at −80°C as well as at −40°C, which proves the excellent low temperature toughness of the developed steel.

3.2 CO_2 Corrosion Resistance

The CO_2 corrosion resistance was evaluated by measuring weight loss in an immersion test under an environment of high temperature and high CO_2 partial pressure. **Figure 5** shows the test results plotted against the test temperature and CO_2 partial pressure. The numeral given to every plot is the corrosion rate. Assuming that a corrosion rate of 0.127 mm/y (5 mpy) is generally acceptable as a standard, the developed material is judged to be suitable under an environment of 160°C and 2.0 MPa CO_2.

3.3 SSC Resistance

The SSC resistance at the welded joint was evalu-

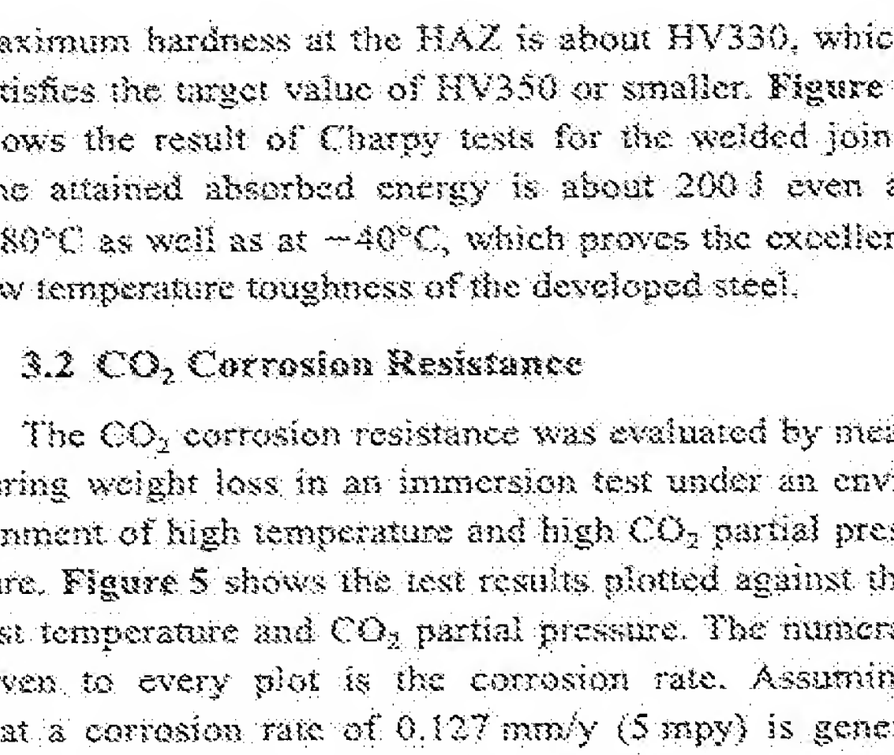

Fig.5 CO_2 corrosion test results of the base metal

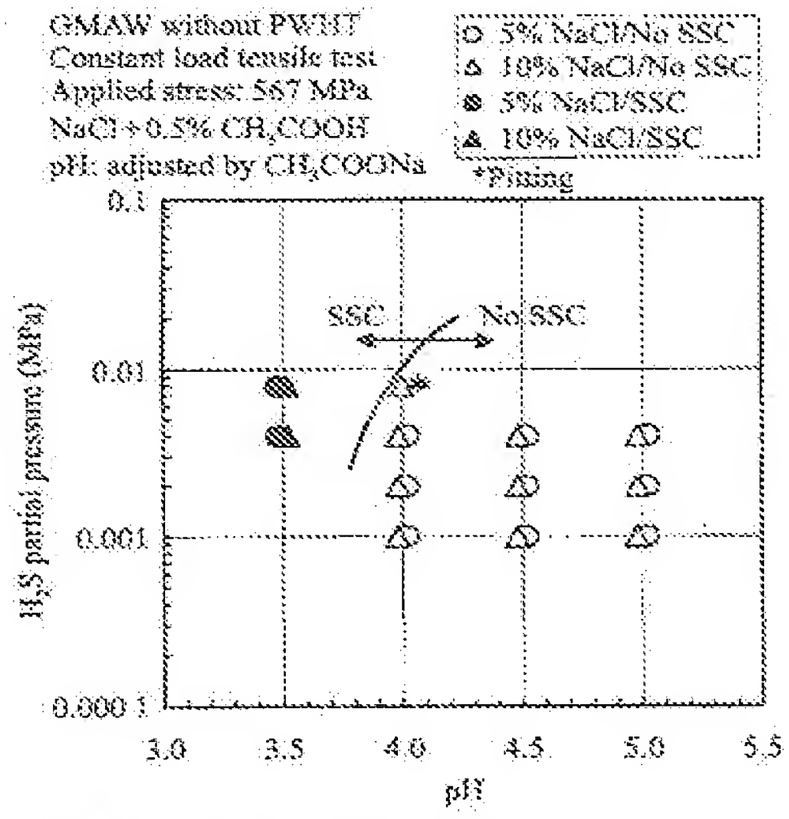

Fig.6 SSC test results of the welded joint

ated by a constant load tensile SSC test. The solution was an aqueous mixture of 5% or 10% NaCl with 0.5% CH_3COOH, and the pH was adjusted in the range from 3.5 to 5.0 using CH_3COONa. The test gas was a mixture of H_2S at partial pressures from 0.001 to 0.007 MPa with the balance of CO_2 to make the total pressure 0.1 MPa. The applied stress was 567 MPa, which is equivalent to 90% of the YS of the base material. **Figure 6** shows the test results plotted against the pH and H_2S partial pressure. As can be seen, although SSC occurred at the HAZ at pH3.5, no SSC occurred under the target environment of pH4.0 and H_2S partial pressure of 0.001 MPa.

4. Intergranular Stress Corrosion Cracking at Girth Weld

According to a recent paper[7], a laboratory study found that intergranular stress corrosion cracking (IGSCC) occurred at the girth weld of a sample having the similar compositions to the developed steel, under a high temperature CO_2 environment. In addition, another paper reported that gas leakage occurred due to IGSCC in an actual pipeline using a material, free from Mo, having the similar compositions to the developed steel[8].

Some results of our investigations on the mechanism of this phenomenon and on preventive measures[9] are described below.

4.1 Mechanism of IGSCC Generation

To identify the effect of welding conditions on the sensitization behavior, SCC tests were conducted using samples which were subjected to two passes of simulated welding thermal cycles. For conducting the tests under severer conditions, the corrosive environment was brought to pH2.0, and the U-bend test method, which

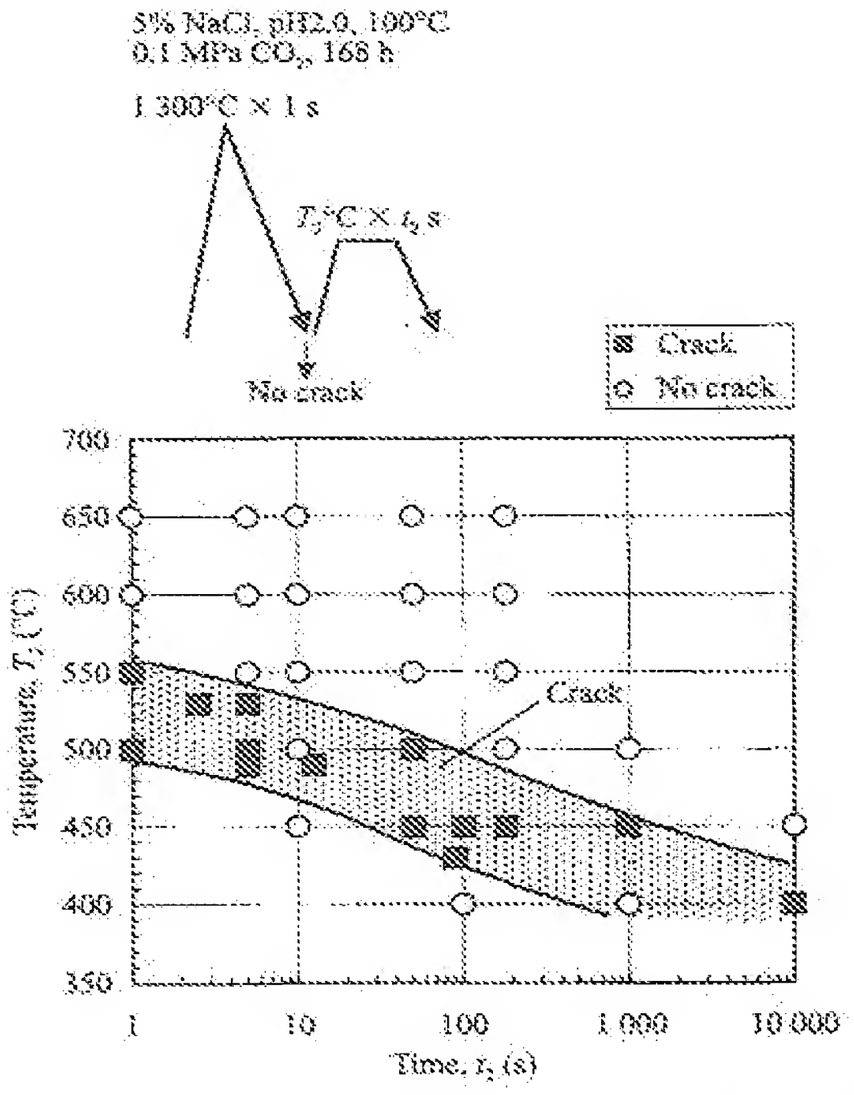

Fig.7 Results of U-bend SCC tests for simulated HAZ

can apply larger strains, was used. Figure 7 gives plots of SCC test results under the second pass condition. The figure shows that some of samples with the second pass thermal cycle suffered cracks. The samples which were subjected only to the first pass did not suffer cracks.

These results suggest that the cause of IGSCC is as follows. When carbon, which is dissolved under high temperature heat cycles, precipitates during the subsequent heat cycle as carbide at the grain boundary of prior-austenite, a Cr-depleted zone forms in the vicinity of the carbide at the grain boundary, thereby sensitizing the material.

4.2 Method to Prevent IGSCC

Since IGSCC is presumably caused by the Cr-depletion zone, potential methods to prevent IGSCC include performing PWHT to diffuse Cr for recovering from Cr depletion, and establishing very low C content and to add Ti for suppressing the precipitation of Cr carbide.

To confirm the effect of PWHT, a material containing 100 ppm of C was sensitized by two passes of heat cycles, followed by a third pass of heat cycles under various conditions. Thus prepared samples were evaluated by the U-bend SCC test similar to that described above. The results are shown in Fig. 8. As shown, the sensitized samples did not suffer cracks after heating to a temperature range from 550°C to 700°C for several minutes. This effect was probably because the heat treatment satisfactorily enhances Cr diffusion, thus diminishing the Cr-depleted zone. IGSCC will be prevented by applying PWHT for a short time, within several minutes, which does not significantly hinder the efficiency of practical pipe-laying.

To confirm the effect of reduction in C content and addition of Ti, materials with various C and Ti contents were evaluated. With the samples treated by a heat cycle of 450°C for 1 000 s, a condition that easily induces sensitization, a U-bend SCC test similar to that applied before was performed. As a severer test condition, samples which had a notch of stress concentration factor 4 at the U-bend section were separately tested. Figure 9

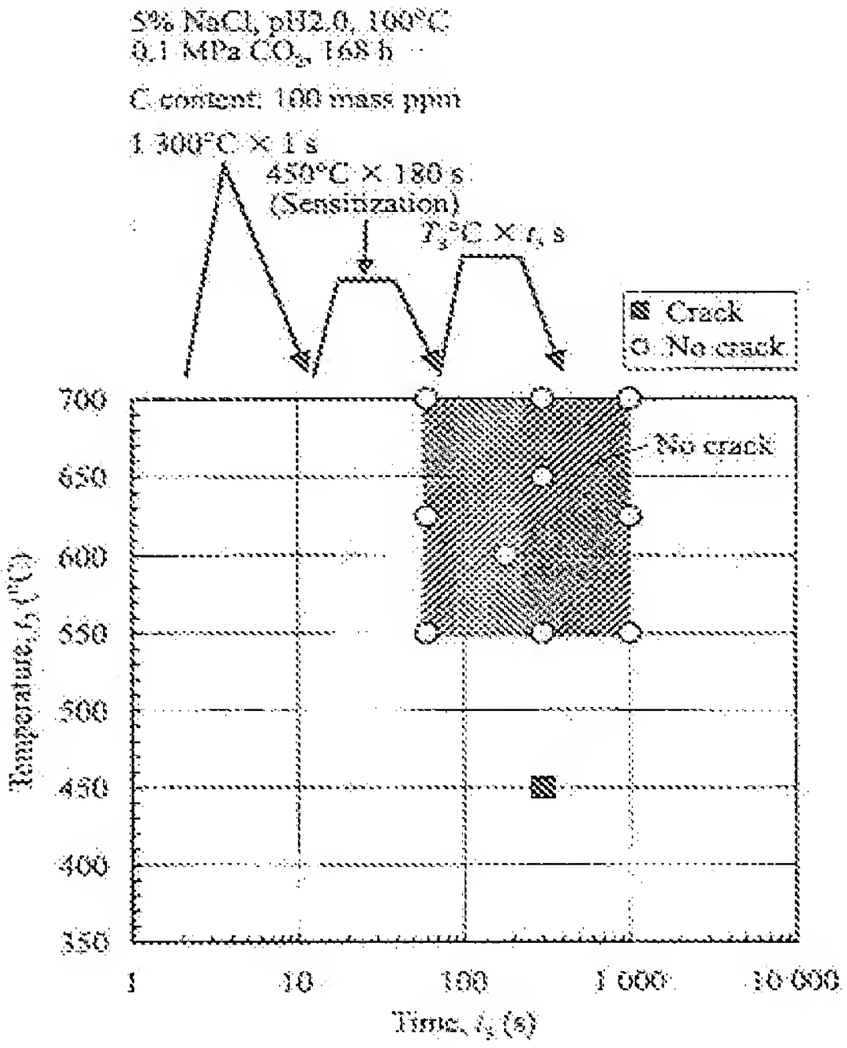

Fig.8 Effects of thermal cycle conditions after sensitization on SCC behavior

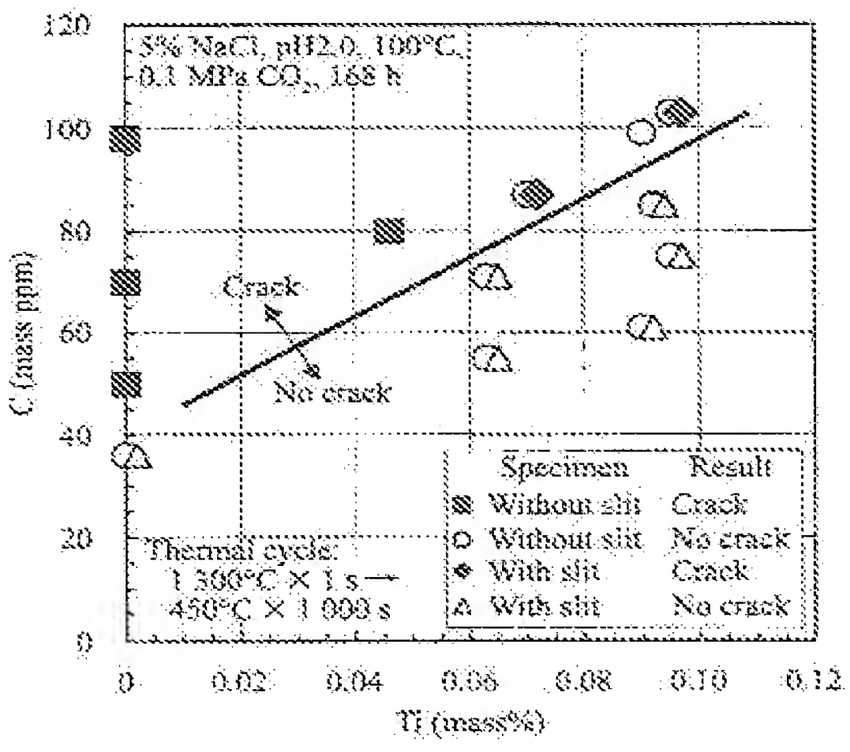

Fig.9 Effects of C and Ti on SCC test results

shows the SCC test results arranged by the C and Ti contents. The figure shows that reduction in C content and addition of Ti suppress the cracks. This is presumably because the suppression of dissolved C during welding and the conversion to Ti carbide suppress the precipitation of Cr carbide which causes Cr depletion. Therefore, reduction in C content and addition of Ti are effective ways of improving the resistance of the material to IGSCC.

5. Conclusion

This paper described the development and characteristics of a seamless steel pipe made of martensitic stainless steel for linepipes, having improved weldability. The weldability of the steel pipe has been improved by decreasing the C and N contents, and the excellent mechanical properties and corrosion resistance have been achieved by the optimization of other alloying elements.

The major characteristics of the steel are given below.

(1) The steel has excellent weldability free from weld cracking even without preheating.

(2) The steel has X80 grade strength, and low temperature toughness of 200 J or larger Charpy absorbed energy at −40°C.

(3) The steel has excellent CO_2 corrosion resistance, giving 0.127 mm/y or smaller corrosion rate under an environment of 160°C and 2.0 MPa CO_2.

(4) The steel has excellent SSC resistance under an environment of pH4.0 and H_2S partial pressure of 0.001 MPa.

(5) Intergranular stress corrosion cracking is prevented by a short period (several minutes) of PWHT. Reduction in C content and addition of Ti are effective to improve the IGSCC resistance of the material.

Since the material has excellent weldability, mechanical properties, and corrosion resistance, its application to pipelines transporting production fluid containing corrosive gases such as CO_2 is expected to be expanded as an economical material with a low life cycle cost.

References

1) van Bodegom, L.; van Gelder, K.; Spaninces, J. A. M. Control of CO_2 corrosion in wet gas lines by injection of glycol. CORROSION/88. paper no. 187, 1988.

2) Ogawa, T.; Koseki, T. Welding technology trend of duplex stainless steels in oil and gas industry application. J. Jpn. Welding Soc. vol. 57, no. 2, 1988, p. 92–99.

3) Watanabe, M.; Mukai, Y. Sutenresukou-no Youseisu. Tokyo, The Nikkan Kogyo Shimbun, 1971, 180 p. (ISBN 4-526-00516-9)

4) Miyata, Y.; Kimura, M.; Murase, F. Development of martensitic stainless steel seamless pipe for linepipe application. Kawasaki Steel Technical Report. no. 38, 1998-04, p. 53–60.

5) Kimura, M.; Miyata, Y.; Kitahaba, Y. Development of new OCTG HP-13Cr with superior CO_2 corrosion resistance and SSC resistance. Kawasaki Steel Technical Report. no. 38, 1998-04, p. 47–52.

6) Miyata, Y.; Kimura, M.; Toyooka, T.; Nakano, Y.; Murase, F. Corrosion performance of weldable 12Cr stainless steel seamless linepipe. EUROCORR/98.

7) Rogne, T.; Lange, H. L.; Svenning, M.; Aldstedt, S.; Solberg, J. K.; Ladanova, E.; Olsen, S.; Howard, R.; Leturno, R. Intergranular corrosion/cracking of weldable 13%Cr steelat elevated temperature. CORROSION/2002. paper no. 02428, 2002.

8) van Gestel, W. Girth weld failure in 13Cr sweet wet gas flow lines. CORROSION/2004. paper no.04141, 2004.

9) Miyata, Y.; Kimura, M.; Nakamichi, H. Sato, K.; Itakura, N.; Masamura, K. Effects of thermal cycle conditions on intergranular stress corrosion cracking in sweet environment for supermartensitic stainless steel. CORROSION/2005. paper no. 05095, 2005.

Paper No.
07092

NACE INTERNATIONAL CORROSION 2007 CONFERENCE & EXPO

Effects of chemical components on resistance to intergranular stress corrosion cracking in supermartensitic stainless steel

Yukio MIYATA and Mitsuo KIMURA
JFE Steel Corporation, Steel Research Laboratories
1-1, Kawasaki-cho, Handa, Aichi, 475-8611, Japan

Katsumi MASAMURA
JFE Steel Corporation, Tokyo Head Office
2-2-3, Uchisaiwai-cho, Chiyoda-ku, Tokyo, 100-0011, Japan

ABSTRACT

Low carbon martensitic stainless steels, called supermartensitic stainless steels (SMSS), have widely been applied for flowlines transporting corrosive oil and gas. However, intergranular stress corrosion cracking (IGSCC) in girth welds of the steel has become a major concern recently. A number of research works have been conducted to clarify the mechanism and to establish the measures. The most likely mechanism of IGSCC is chromium depletion on grain boundary because it is observed in lean grade SMSS, which contains no molybdenum. However, neither depletion nor carbide of chromium has been detected so far in 2-3% Mo-added high grade SMSS, although the steel suffers IGSCC under some conditions. In order to clarify the mechanism in high grade steel, effects of chemical components on IGSCC resistance were investigated. Simulated HAZ specimens with various conditions of thermal cycles were tested in hot acid environments by U-bend SCC test. The test results showed that reduction of carbon and addition of titanium are effective to improve the resistance to IGSCC. Both would inhibit to form chromium carbide that causes to chromium depletion. Therefore, it suggests that the mechanism of IGSCC in high grade SMSS is chromium depletion, as in lean grade.

Keywords: supermartensitic stainless steel (SMSS), intergranular stress corrosion cracking (IGSCC), sensitization, stress corrosion cracking (SCC), linepipe, girth welding, heat affected zone (HAZ), carbide, chromium depletion

Copyright
©2007 by NACE International. Requests for permission to publish this manuscript in any form, in part or in whole must be in writing to NACE International, Copyright Division, 1440 South creek Drive, Houston, Texas 777084. The material presented and the views expressed in this paper are solely those of the author(s) and are not necessarily endorsed by the Association. Printed in the U.S.A.

INTRODUCTION

Low carbon martensitic stainless steels, which are called supermartensitic stainless steels (SMSS), have been developed for linepipes under sweet environments since the late 1990's [1]-[3]. They have contributed to oil and gas industry as alternative materials for duplex stainless steels or carbon steel with inhibitor [4]-[8].

However, new type of cracking of the steel has been reported on the basis of laboratory tests [9], [10]. The cracking occurs in the heat affected zone (HAZ) of girth welds and its morphology is intergranular stress corrosion cracking (IGSCC). In-service failure caused by same type of cracking has also been reported in lean grade SMSS, which contains no molybdenum [11]. No experience of in-service failure has been reported in high grade SMSS, which contains 2-3% of molybdenum. The most likely mechanism of the IGSCC is chromium depletion on grain boundary accompanied by re-precipitation of chromium carbide during girth welding. The fact that chromium depletion was observed in lean grade SMSS [12] supported the idea. However, no clear evidence has been obtained so far in high grade SMSS. In order to clarify the mechanism in high grade SMSS, effects of chemical components such as C and Ti on resistance to IGSCC were studied. This paper describes the results of the study.

EXPERIMENTAL PROCEDURES

Materials

High grade SMSS with various content of carbon and titanium were prepared for the study. The compositions of the steel used are shown in Table 1. Each ingot in 50 kg weight was hot-rolled into 15 mm thickness sheet followed by quenching and tempering.

HAZ simulation

The steels were subjected to thermal cycles for HAZ simulation by Gleeble tester. The specimens for the HAZ simulation were smoothly machined and their dimension was 4 mm thick and 15 mm wide, as shown in Figure 1 (a). The thermal cycles basically consisted of two heat passes. It is based on the process of re-precipitation of chromium carbide causing chromium depletion, which means that chromium carbides are dissolved during higher temperature pass and re-precipitate during following lower temperature pass. The first pass was heated to 1300 °C for 1 s. The conditions of the second pass were varied in the temperature of 400 to 650 °C and the holding time of 3 to 10000 s. The rate of cooling on thermal cycle was adjusted by nitrogen gas blow. Cooling time from 800 to 500 °C was 9 s, which was corresponding to 1.0 kJ/mm of heat input with 12.7 mm thickness plate.

SCC tests

In the previous paper [12], the U-bend SCC test in lower pH environment was found to be an appropriate method for the evaluation of IGSCC for SMSS. The specimens for U-bend SCC test were machined into 2 mm of thickness from the sample after thermal cycles by Gleeble tester. U-bend test

method was basically according to ASTM G30. Some of U-bend SCC test were conducted under the condition with a notch for a more severe evaluation. The dimension of the notch was 2 mm width and maximum 3 mm depth with 1 mm radius, as shown in Figure 1 (b).

For the evaluation of the effect of thermal cycle conditions on the susceptibility to IGSCC, lower pH was selected as environmental conditions, namely 5% NaCl, pH 2.0 aqueous solution with 1 bar CO_2 at 100 ℃. The pH was adjusted by HCl addition. Carbon dioxide gas was continuously bubbled through the solution during the test. The test duration was 168 h. For the evaluation of the dependence of environmental conditions such as temperature and pH, higher CO_2 partial pressure and higher NaCl content were selected as environmental conditions, namely 20 % NaCl, 15bar CO_2, 100-150 ℃, pH 2.0-5.0. The pH was adjusted by HCl or $NaHCO_3$ addition. The test duration was 720 h.

Figure 2 shows an example of crack resulted in U-bend SCC test. Because the crack shows intergranular fracture, this test method would be appropriate for the simulation of actual cracking.

RESULTS

SCC test results for steels with various content of C and Ti

The results of the SCC tests for the steel with 98 ppm of C and no Ti addition are plotted as a function of temperature and holding time of the second pass as shown in Figure 3. The conditions of the first pass was 1300 ℃ for 1 s. Cracks were recognized in temperatures of 450 to 550 ℃ and holding time of 3 to 100 s for the second pass. And cracks were also recognized in longer holding time at lower temperatures. No crack occurred in longer holding time at higher temperatures or shorter holding time at lower temperatures. Figure 4 shows the test results for the steel with 70 ppm of C and no Ti addition. Cracks in the steel occurred more limited conditions of thermal cycle than those in the steel with 98 ppm of C. Figure 5 shows the test results for the steel with 36 ppm of C and no Ti addition. No crack was observed in any thermal cycle conditions tested. Therefore, it was clarified that reduction in C content of steel is effective to improve the resistance to IGSCC.

The results of SCC tests for the steel with 0.046 % of Ti are shown in Figure 6. Crack was recognized in the conditions of 450 ℃ for 1000 s for the second pass of thermal cycle. Any crack was not recognized in the other thermal cycle conditions. Figure 7 shows the test results for the steel with 0.090 % of Ti. No crack was observed in any thermal cycle conditions tested. Therefore, it was clarified that Ti addition to steel was effective to improve the resistance to IGSCC.

The results of U-bend tests are plotted as a function of C and Ti content in Figure 8. Since the most severe second pass conditions as susceptibility to IGSCC seemed to be 450 ℃ for 180 or 1000 s based on the SCC test results as shown in Figure 4 and 6, these conditions were selected for the evaluation. Moreover, some U-bend tests were conducted with a notch for more severe SCC test condition. Occurrence of crack was prevented by a reduction of C or an addition of Ti.

SCC test results under various environmental conditions

For the evaluation of the dependence of environmental conditions such as temperature and pH, U-bend SCC test were conducted under various temperature and pH conditions at higher CO_2 partial pressure and higher NaCl content. The results of the SCC tests for the steel with 98 ppm of C and no Ti addition are shown in Figure 9. Cracks were observed in the steel under the conditions of 125 ℃

or higher, and 100 °C at lower pH of 2.0. On the other hands, no crack was observed in the steel with 61 ppm of C and 0.046 % of Ti even under the conditions of 150 °C, as shown in Figure 10. Therefore, it was clarified that steel with lower C and higher Ti content is more resistant to IGSCC and can be applied more severe environmental conditions.

DISCUSSION

Effect of C and Ti on resistance to IGSCC

In order to clarify the effects of Ti addition on resistance to IGSCC, analyses of precipitates by electrolytic extraction were conducted for steels with and without Ti. The results are summarized in Table 2. In the steels after sensitized treatment of 1300 °C for 1 s and 500 °C for 50 s, neither precipitate of Fe, Cr, Mo nor Ti was observed, against more than each 100 ppm of precipitate in the steel before sensitized treatment (base metal). The result of X-ray diffraction of the extracted residue for the Ti less steel before sensitized treatment is shown in Figure 11 (a). Only $M_{23}C_6$ was observed in the residue. This suggests that 764 ppm of Cr precipitates as Cr carbide in $M_{23}C_6$ type. In the residue for the Ti added steel before sensitized treatment, less Cr precipitation was observed than in that for the Ti less steel. And TiN, TiC and intermetallic phase (Laves phase, Fe_2Mo) are observed instead of $M_{23}C_6$, as shown in Figure 11 (b).

Results of thermodynamical calculation for precipitation phase in Ti less and added steels are shown in Figure 12. In the Ti less steel, $M_{23}C_6$ are dissolved at more than 800 °C. On the other hand, TiC and TiN are stable thermodynamically in the Ti added steel instead of $M_{23}C_6$. And carbide as TiC in the Ti added steel is stable at higher temperature than that as $M_{23}C_6$ in the Ti less steel. That is to say, it is hard in the Ti added steel to precipitate $M_{23}C_6$ type carbide and to form dissolved carbon also from a thermodynamical point of view.

Although no carbide is observed in the Ti less steel after sensitization treatment, it is believed that tiny amount of Cr carbides exists on grain boundary and it causes to Cr depletion. Regarding the Ti added steel, no carbide is observed after sensitization treatment, as shown in Figure 11 (c). However, tiny amount of carbide may also exist on grain boundary. This is supported by the fact that crack was observed in the steel with 0.09 % of Ti and 100 ppm of C. It is considered that thermodynamical equilibrium can not strictly be applied to such short time process of welding, especially on grain boundary. However, thermodynamical stability of TiC is predominantly higher than that of $Cr_{23}C_6$. So that leads to preferential precipitation of TiC despite lower content of Ti than that of Cr.

In these discussions, schematic diagram of carbide precipitation during welding for both Ti less and added steels is considered as shown Figure 13 (a) and (b), respectively. The figures (A) show the image of the state before welding. In the Ti added steel, small amount of $Cr_{23}C_6$ may exist as well as TiC as a main carbide. The figures (B) show the image of the state after exposure to a high temperature cycle. The horizontal axis shows the position in welds, in other words, the peak temperature of the first thermal cycle. More amount of C dissolves easily in the position subjected to higher temperature cycle. Less amount of C are dissolved in Ti added steel than in Ti less steel during a high temperature cycle. It is referred from lower solubility of TiC into steel than that of $M_{23}C_6$, as shown in Figure 12. The figures (C) show the image of the state after the whole welds is exposed to a low temperature cycle. In the Ti less steel, tiny amount of $Cr_{23}C_6$ would re-precipitate to cause Cr

depletion. In the Ti added steel, carbide would re-precipitate preferentially as TiC, although very tiny amount of $Cr_{23}C_6$ may also re-precipitate. As a result, less amount of $Cr_{23}C_6$, which leads to Cr depletion, re-precipitate in Ti added steel than in Ti less steel during a low temperature cycle. Therefore, Ti added steel would be hard to form Cr depletion and have higher resistance to IGSCC.

Mechanism of IGSCC in high grade SMSS

The results of the SCC tests in this study showed that crack in the steels with lower C or higher Ti contents occurred under more limited thermal cycle conditions, and more limited environmental conditions. In other words, reduction of C and addition of Ti is effective to prevent IGSCC. This suggests that the cause of IGSCC in the high grade SMSS is also the Cr depletion same as the lean grade SMSS, although no clear evidence of Cr depletion has been recognized in the high grade SMSS.

CONCLUSIONS

In order to clarify the mechanism of intergranular stress corrosion cracking (IGSCC) of high grade supermartensitic stainless steel (SMSS), effects of carbon and titanium on resistance to IGSCC were studied. The results of the SCC tests showed that the reduction of C and the addition of Ti are effective to improve the resistance to IGSCC. Reduction of carbon and addition of titanium would inhibit to form chromium carbide that causes to chromium depletion. Therefore, although neither depletion nor carbide of chromium has been detected so far in the sensitized high grade SMSS, it suggests that the mechanism of IGSCC in high grade SMSS is chromium depletion, as in lean grade.

REFERENCES

1. M. Ueda, H. Amaya, K. Kondo, K. Ogawa and T. Mori, Corrosion 96, Paper No.58, (1996).
2. Y. Miyata, M. Kimura and F. Murase, Kawasaki Steel Technical Report, 38(1998) 53.
3. K. Nose, H. Asahi, H. Tamehiro and H. Inoue, Proceedings of the 16th International Conference on OMAE, 3(1997) 107.
4. T. Barnett, Eurocorr98, (1998).
5. S. A. Duthie, Offshore Technology Conference, OTC8716, (1998).
6. K. van Thoor, Stainless Steel World November 1999, (1999) 42.
7. P. E. Kvaale and S. Olsen, Stainless Steel World 99 Conference, SSW99-202, (1999) 19.
8. E. Warren and J.Bowers, Stainless Steel World March 2003, (2003) 50.
9. T. Rogne and M. Svenning, Supermartensitic Stainless Steels 2002, No.P024 (2002).
10. E. Ladanova, J. K. Solberg and T. Rogne, Supermartensitic Stainless Steels 2002, No.P028 (2002).
11. Gregori, P. Woollin and W. van Gestel, Stainless Steel World December 2003, (2003) 17.
12. Y. Miyata, M. Kimura, H. Nakamichi, K. Sato, N. Itakura and K. Masamura, Corrosion2005, Paper No.05095, (2005)

Table 1 – Chemical compositions of steels used

(mass%)

C (ppm)	Cr	Ni	Mo	Ti	N (ppm)
36-103	12	5.2	2.0	0-0.095	60-80

Table 2 – Results of electrolytic extraction for steels with and without Ti

Material		Thermal history	Precipitation (ppm)			
C	Ti		Fe	Cr	Mo	Ti
98ppm	0.00%	Base metal	387	764	716	-
		Sensitized treatment	<1	<1	<1	-
33ppm	0.09%	Base metal	527	149	658	384
		Sensitized treatment	<1	<1	<1	100

Sensitized treatment: 1300°Cx1s-500°Cx50s

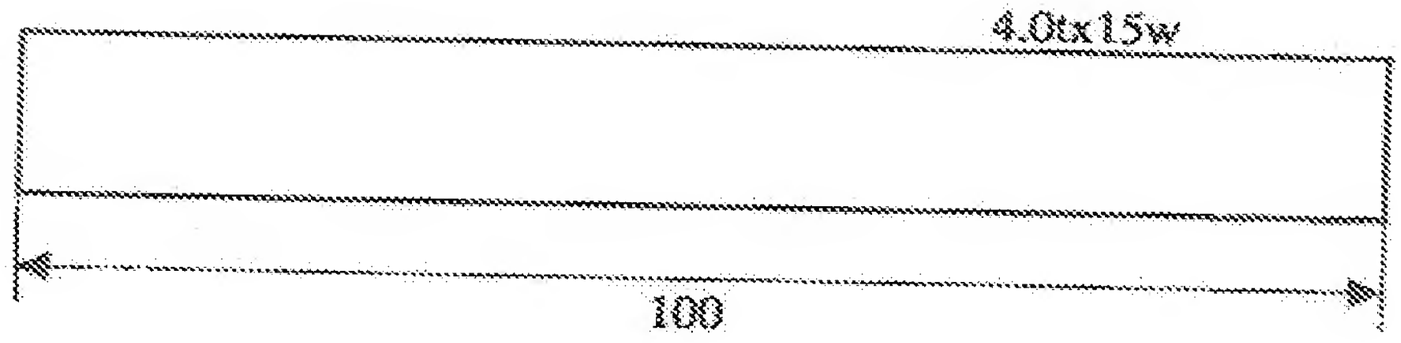

(a) Thermal cycle specimen

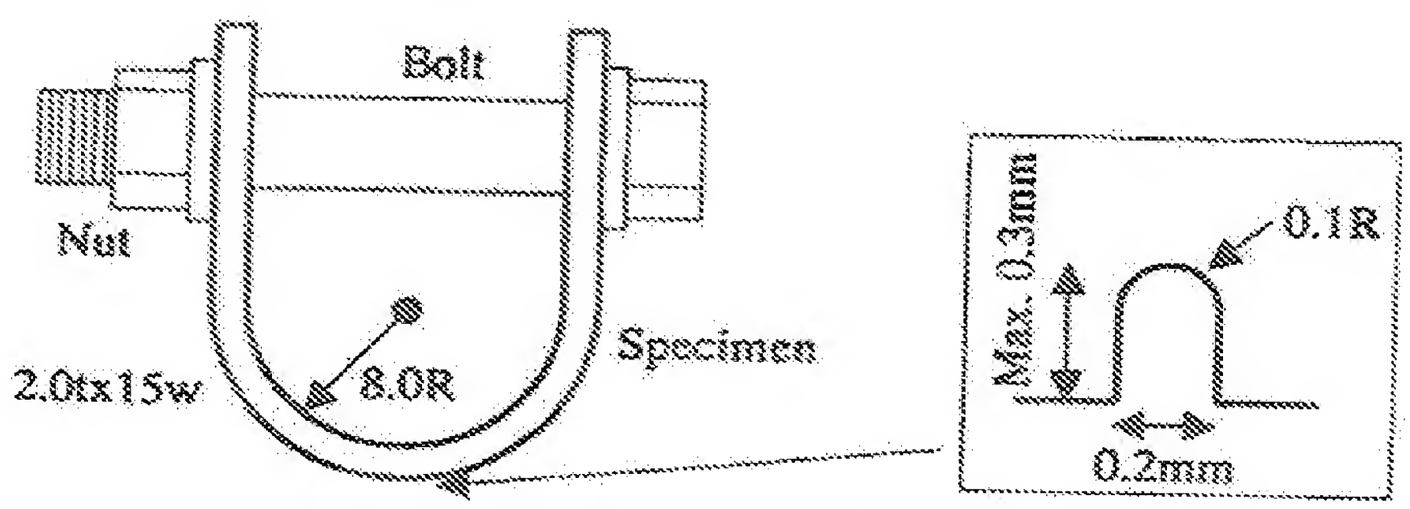

(b) U-bend specimen with and without notch

FIGURE 1 - Schematic Illustration of specimens

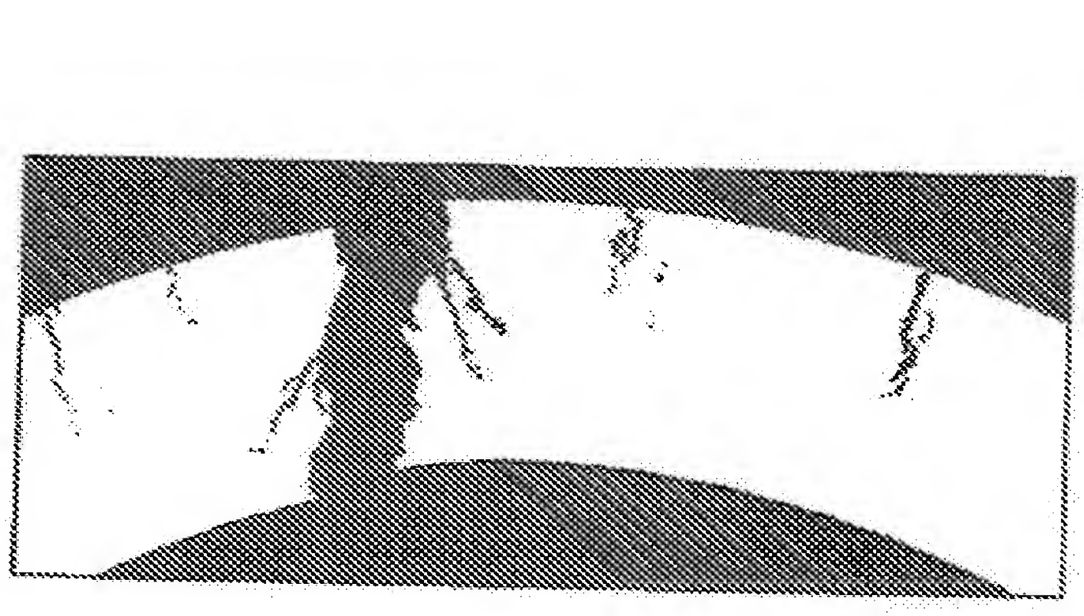

(a) Cross sectional view of specimen

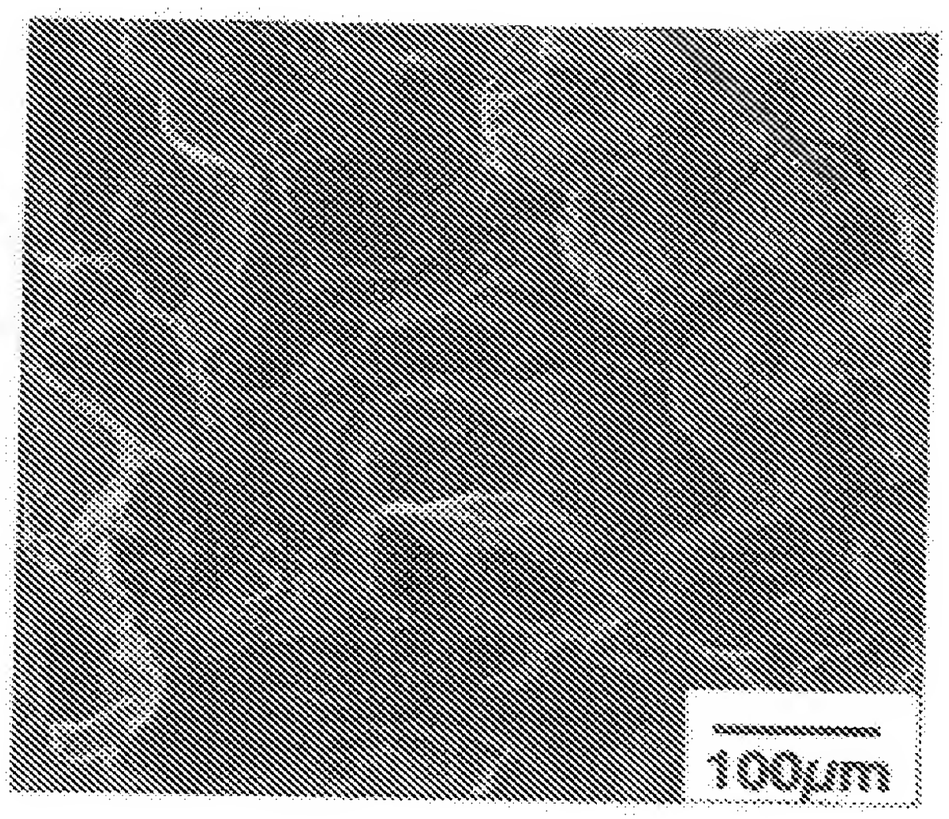

(b) Fracture surface

FIGURE 2 – Crack after U-bend SCC test

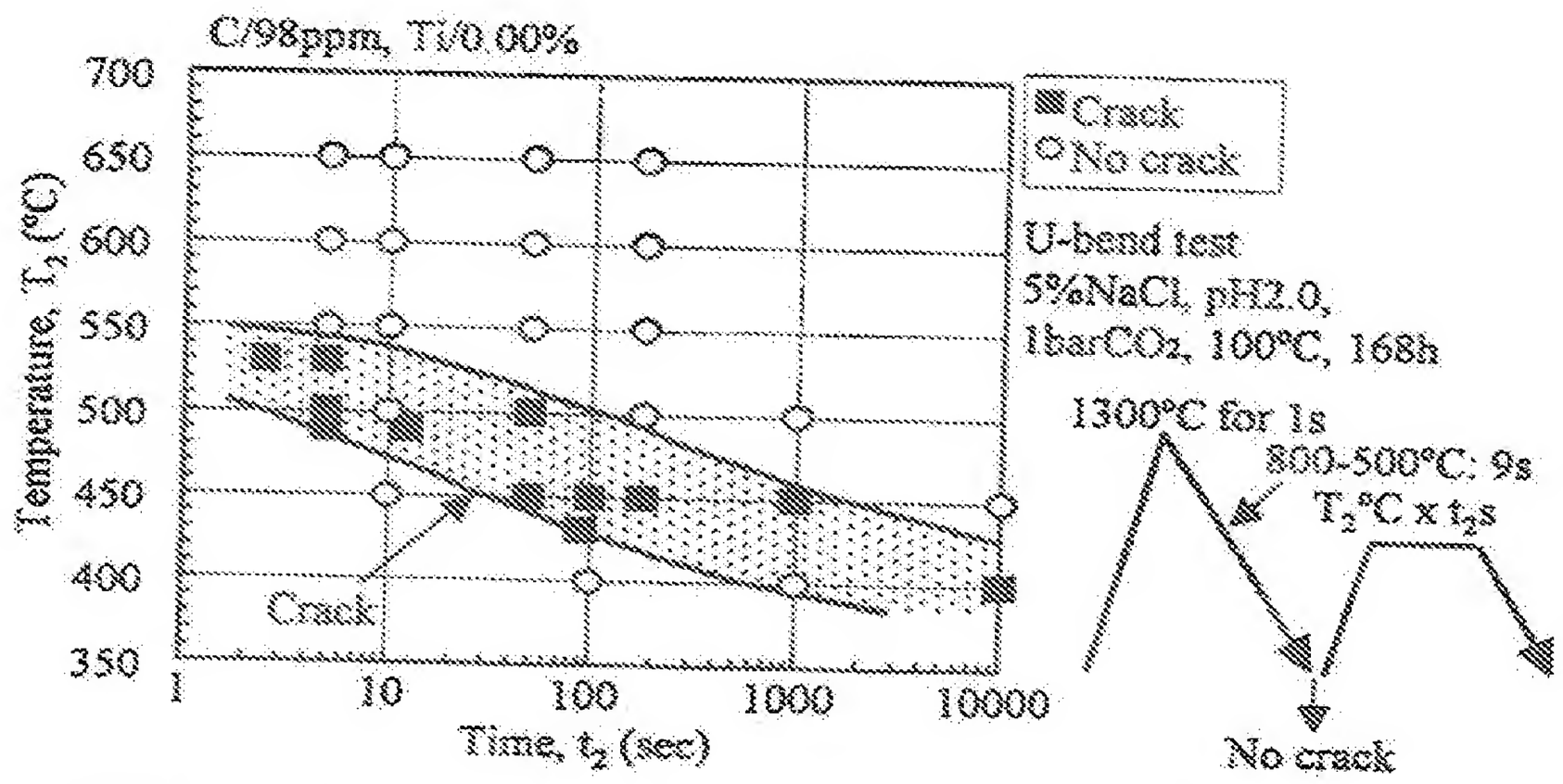

FIGURE – 3 Results of U-bend SCC tests for simulated HAZ of C/98ppm steel

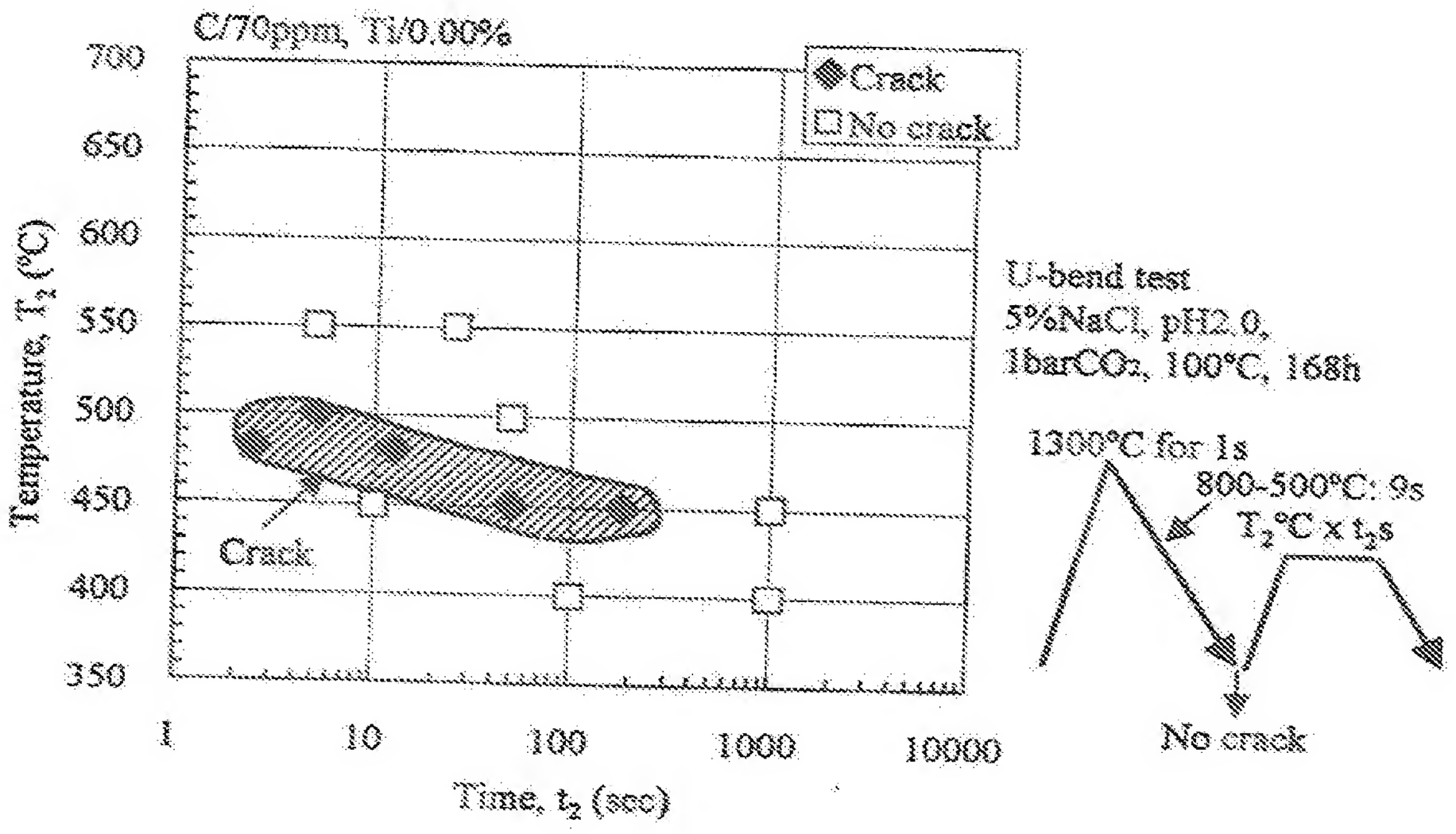

FIGURE – 4 Results of U-bend SCC tests for simulated HAZ of C/70ppm steel

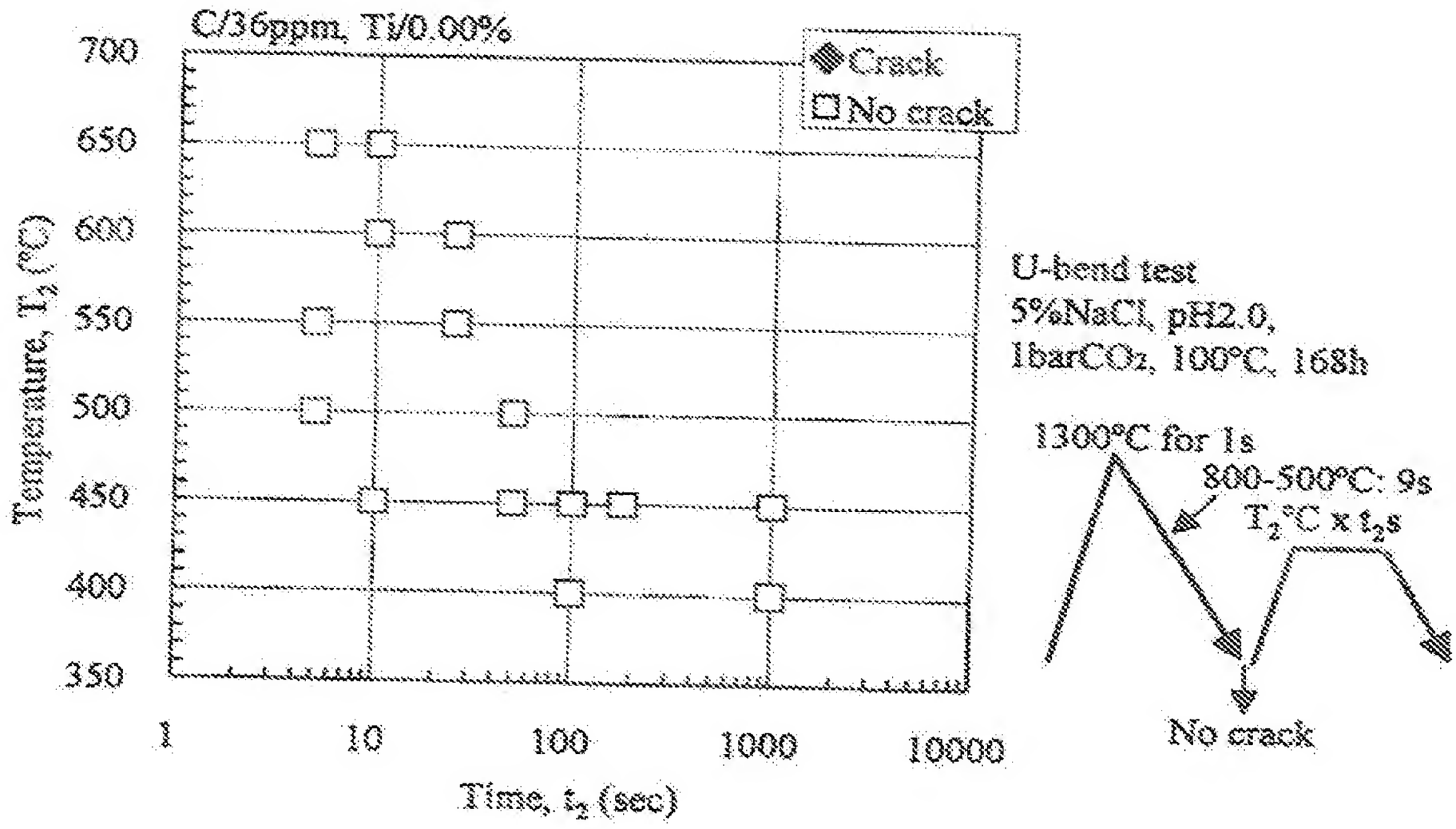

FIGURE – 5 Results of U-bend SCC tests for simulated HAZ of C/36ppm steel

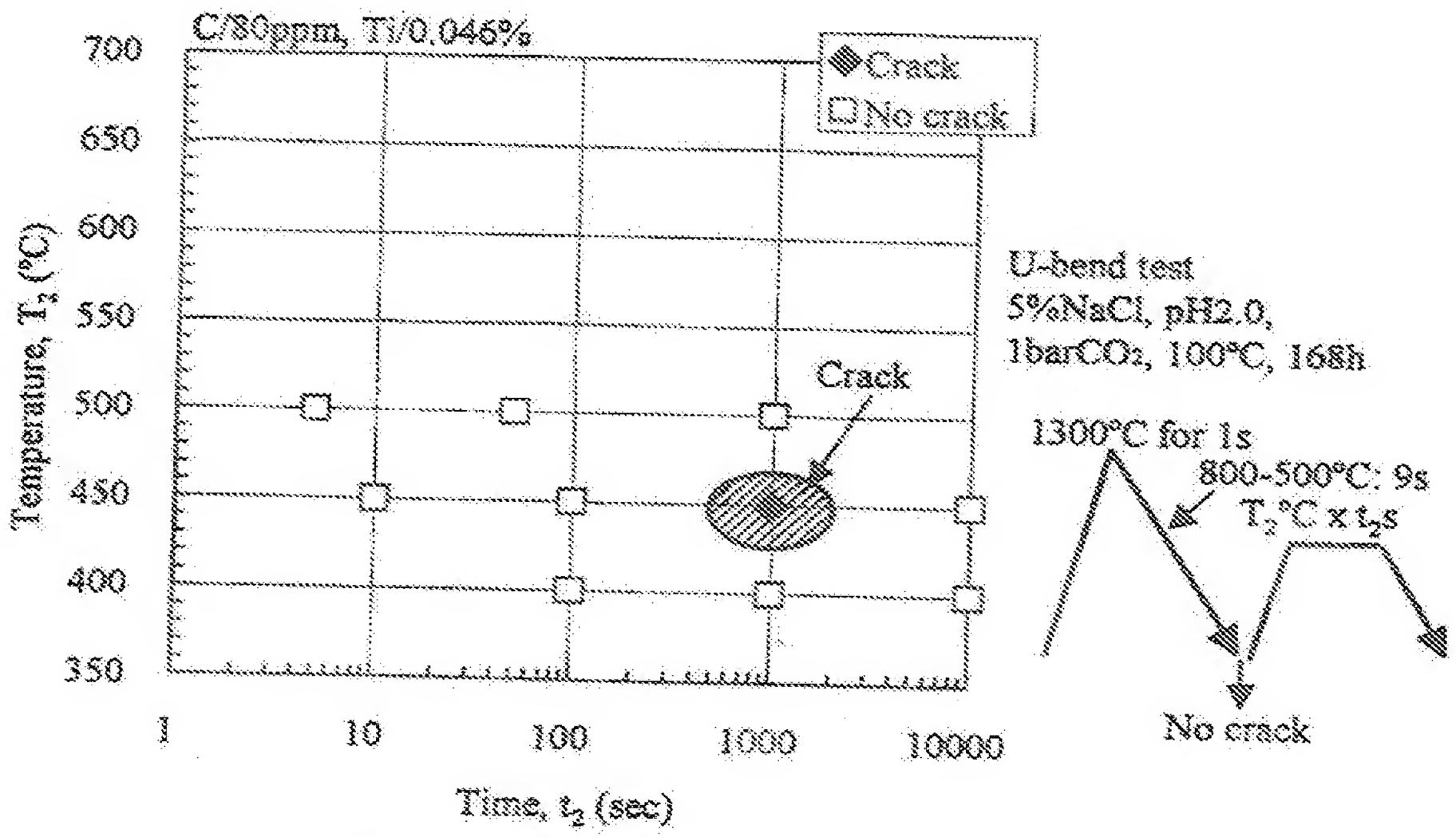

FIGURE – 6 Results of U-bend SCC tests for simulated HAZ of C/80ppm, Ti/0.046% steel

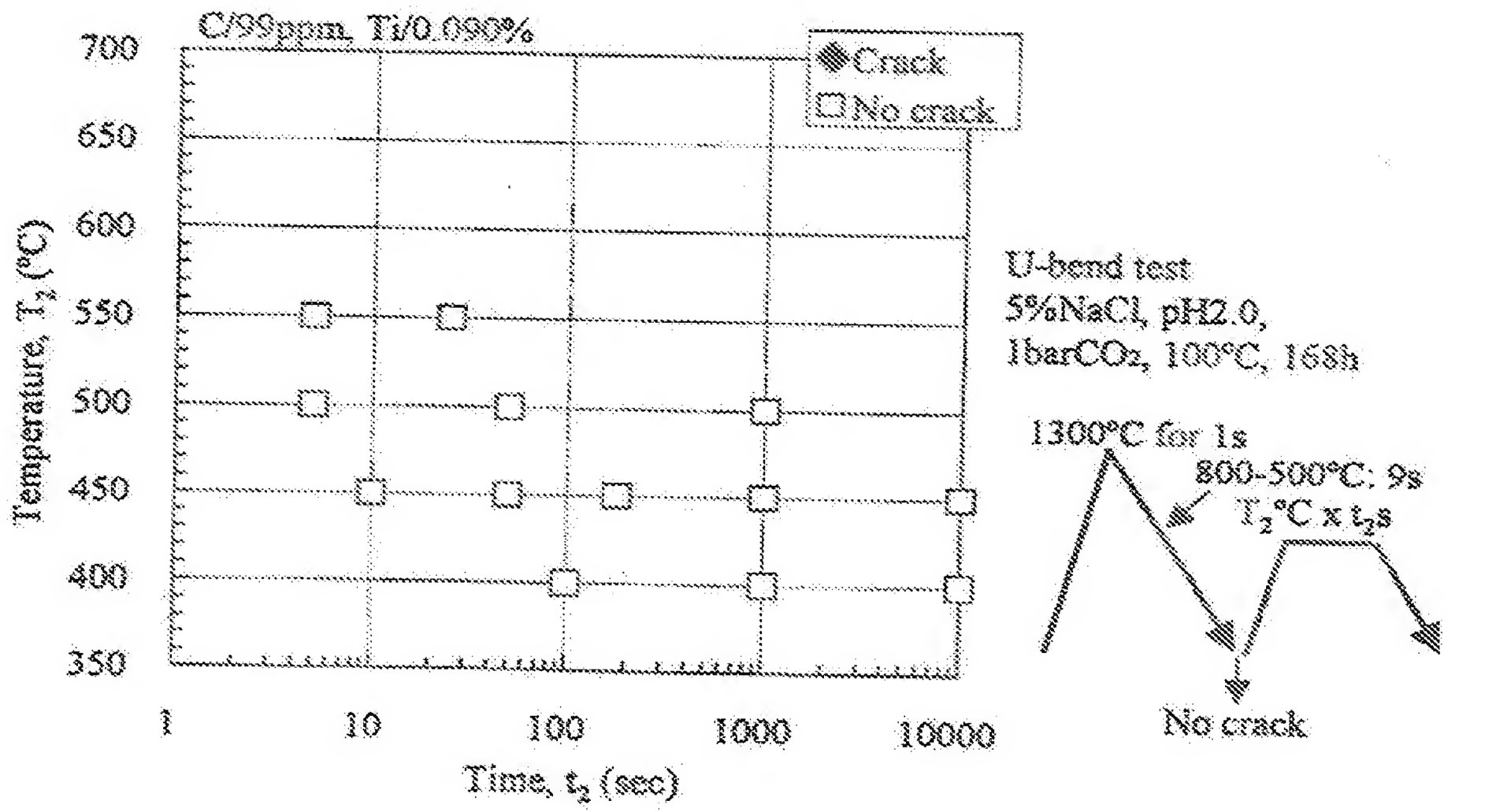

FIGURE – 7 Results of U-bend SCC tests for simulated HAZ of C/99ppm, Ti/0.090% steel

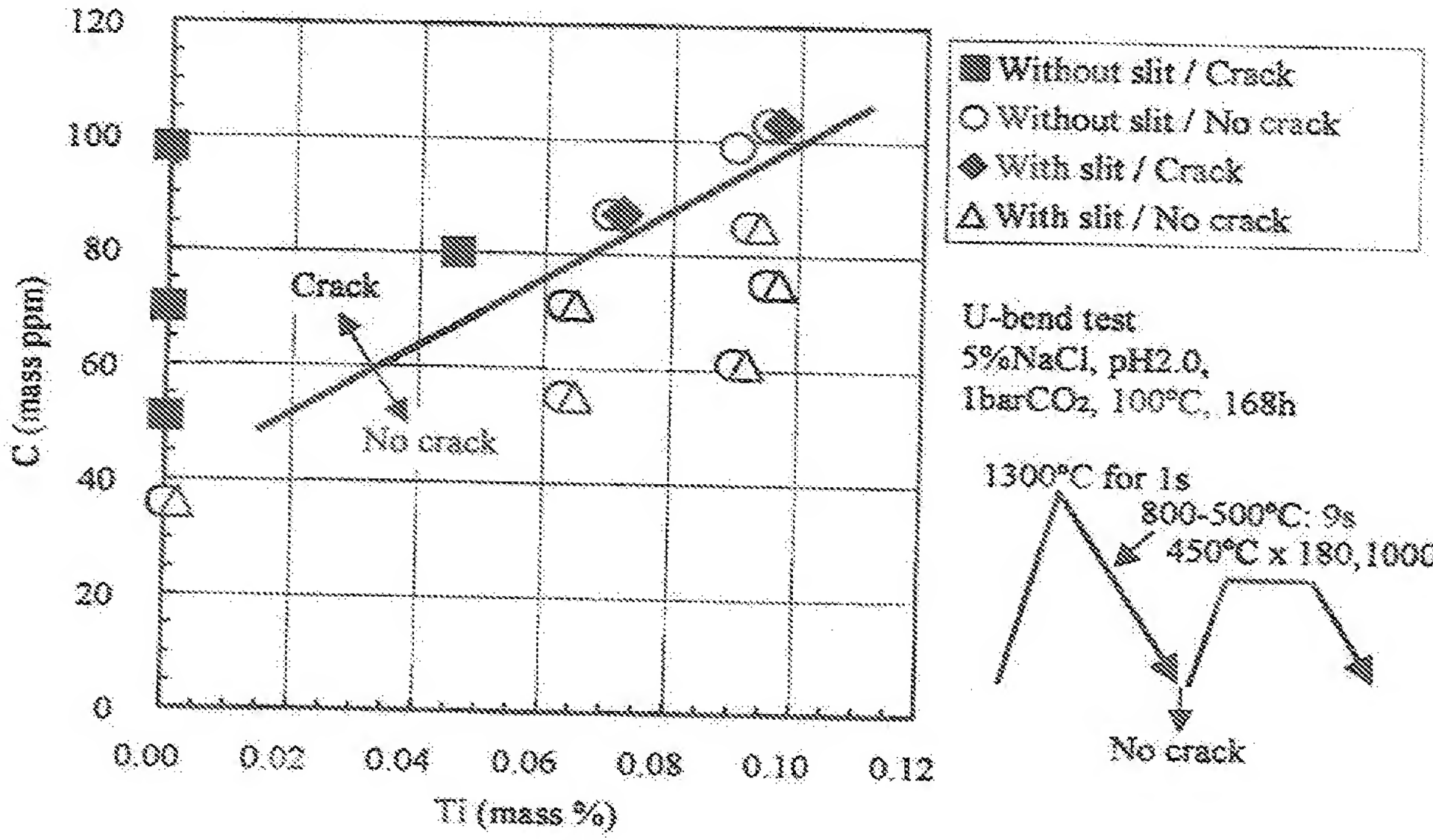

FIGURE – 8 Effects of C and Ti on U-bend SCC tests results

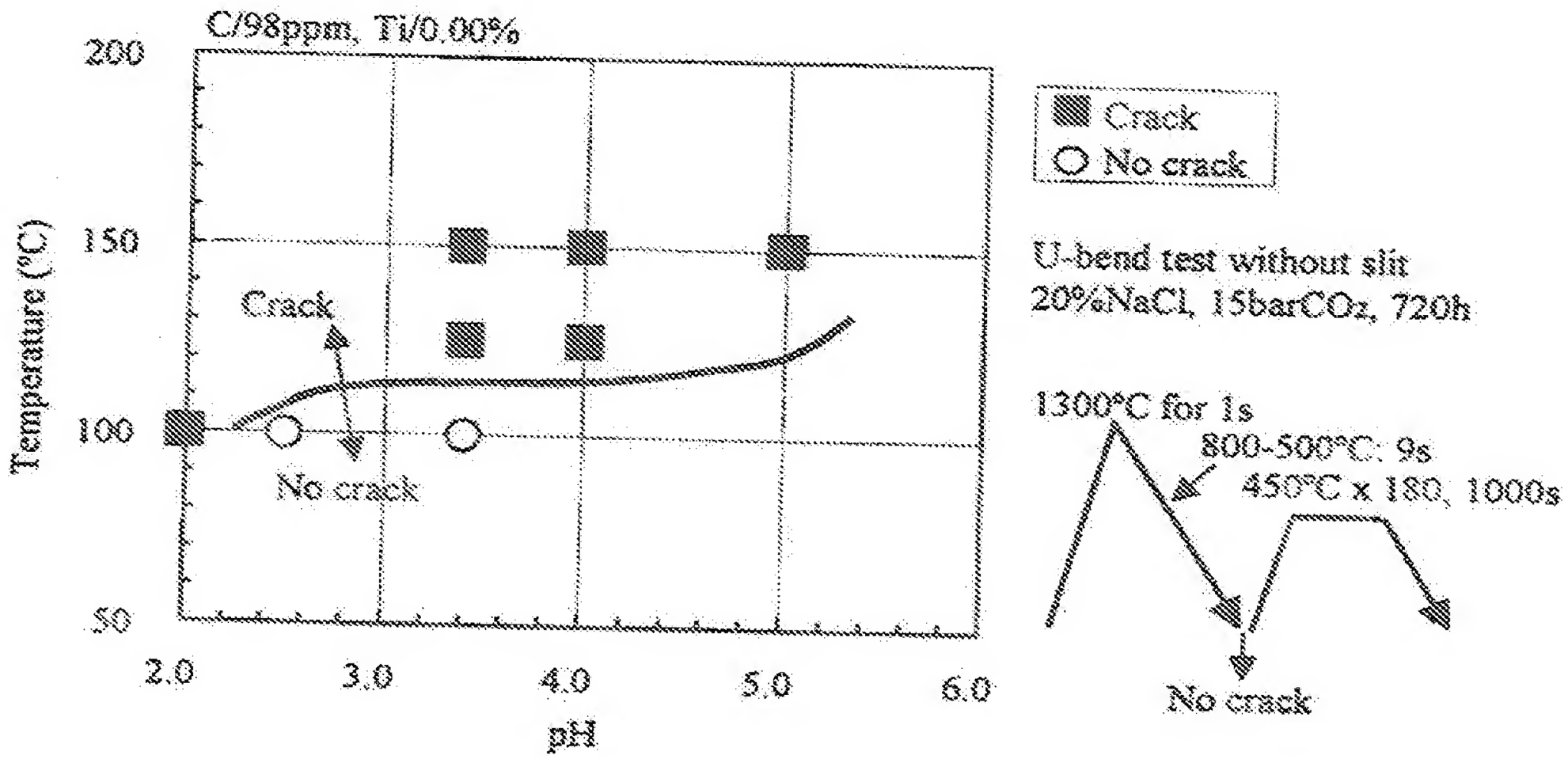

FIGURE – 9 Effects of pH and temperature on U-bend SCC test results for simulated HAZ of C/98ppm, Ti/0.00% steel

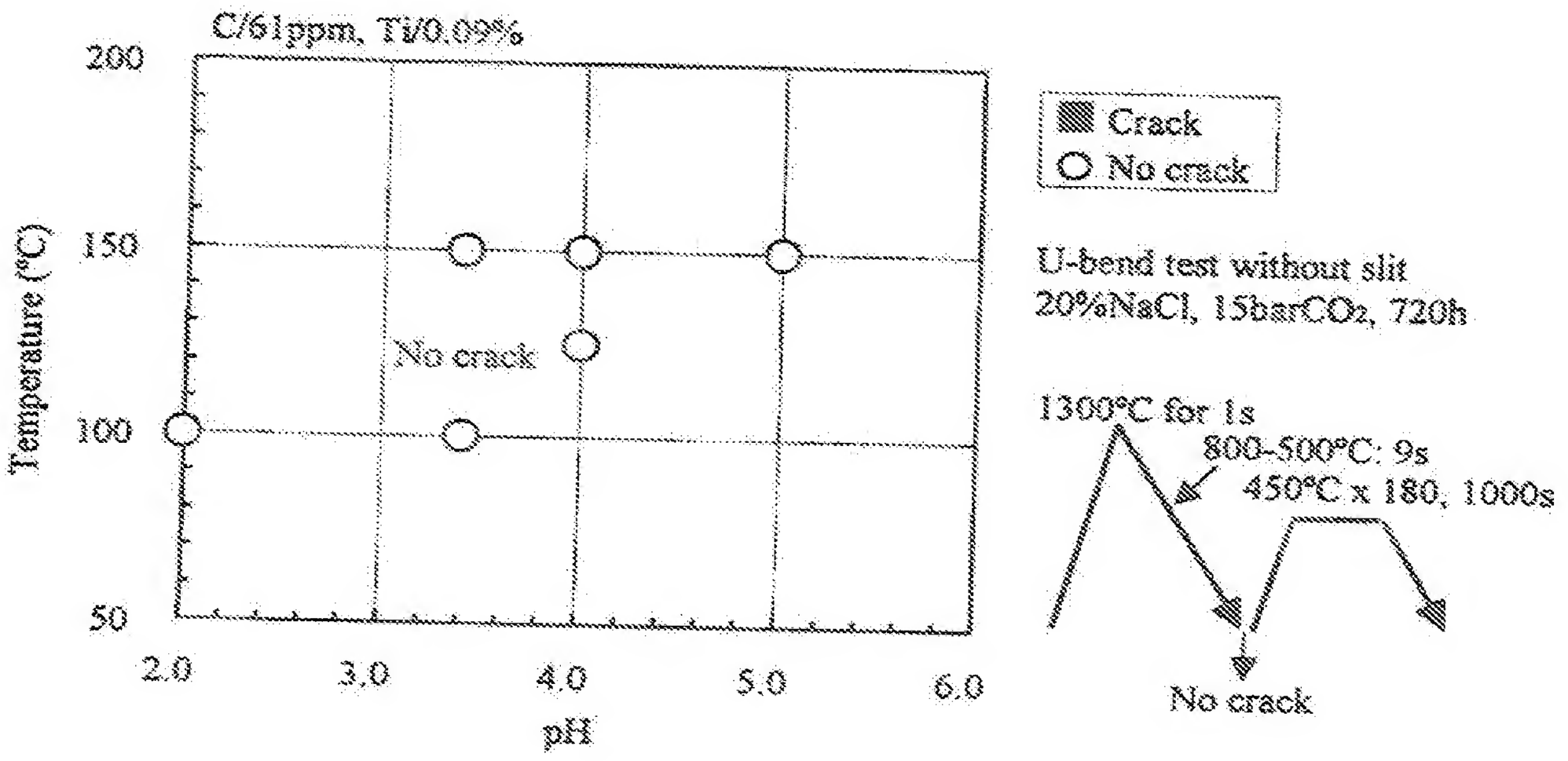

FIGURE – 10 Effects of pH and temperature on U-bend SCC test results for simulated HAZ of C/61ppm, Ti/0.09% steel

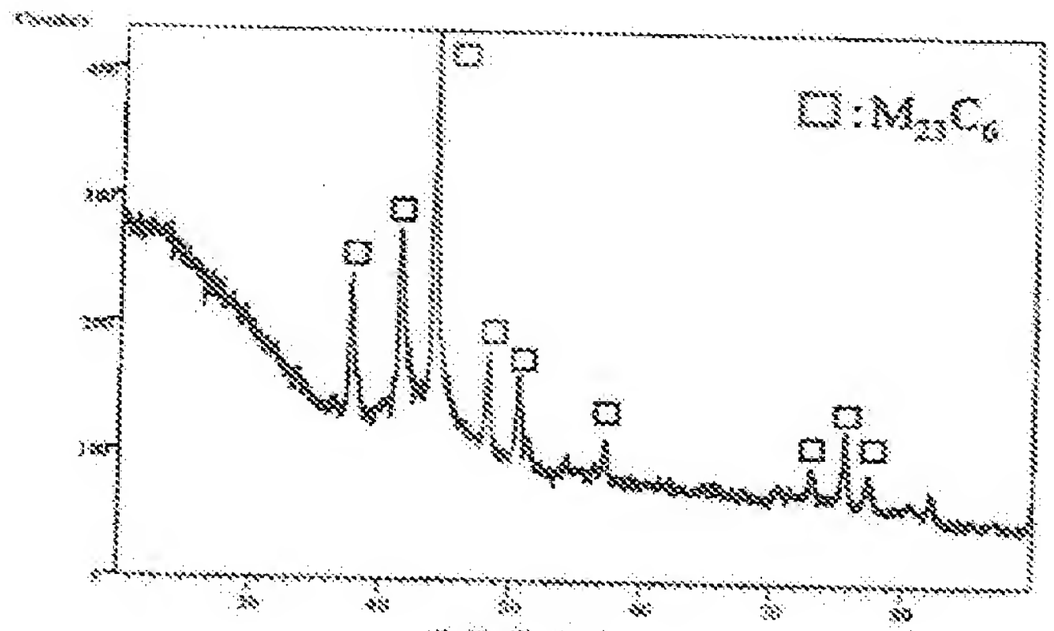

(a) C/98ppm, Ti/0.00% steel
Before sensitized treatment

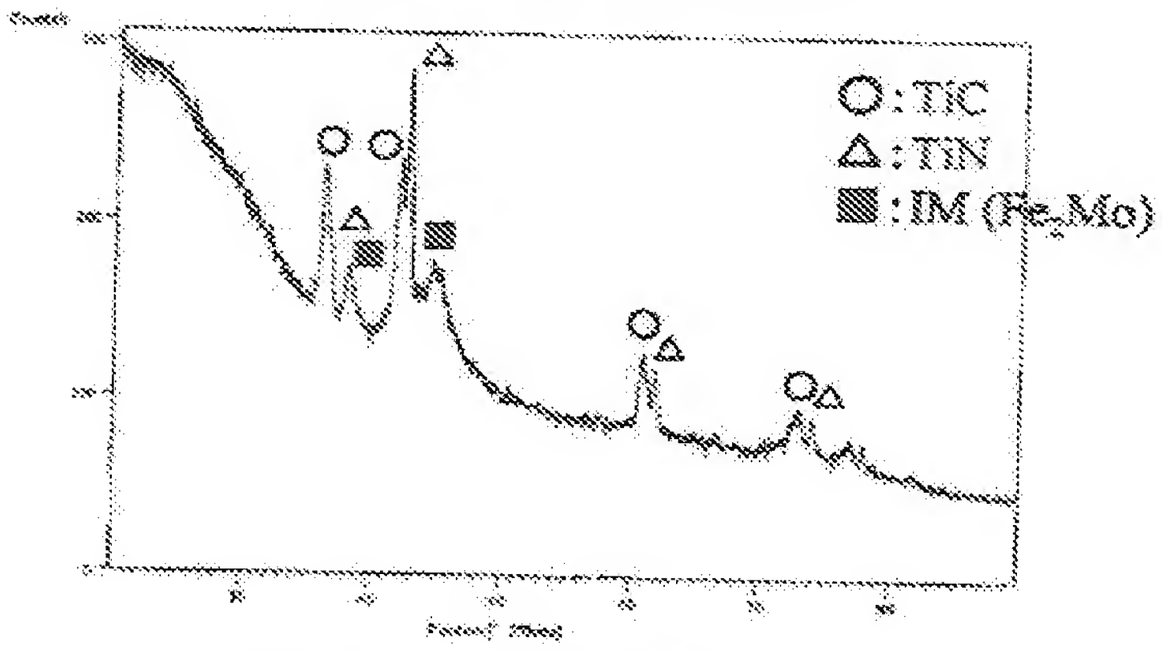

(b) C/99ppm, Ti/0.09% steel
Before sensitized treatment

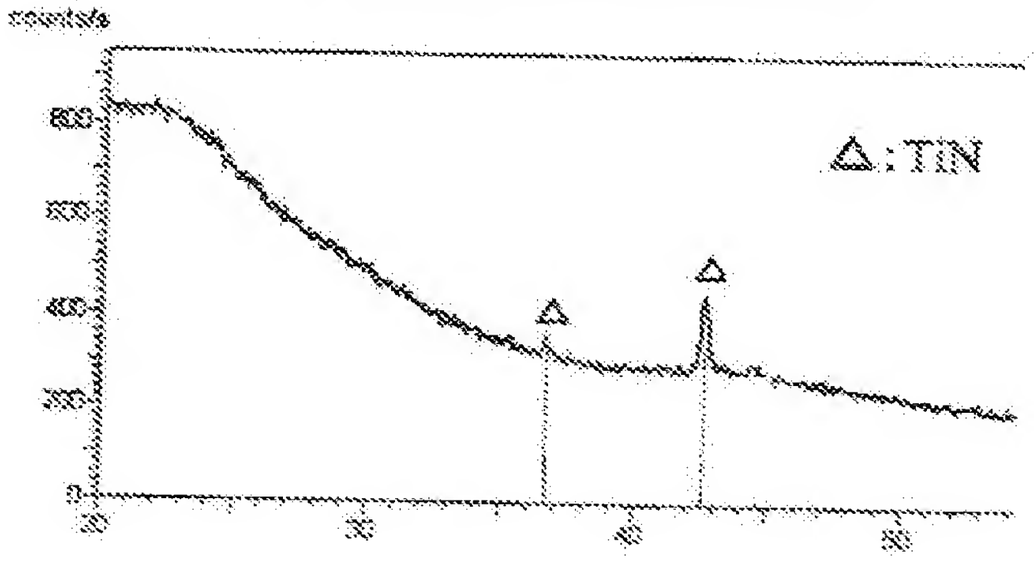

(c) C/99ppm, Ti/0.09% steel
After sensitized treatment (1300°Cx1s- 500°Cx50s)

FIGURE – 11 X-ray diffraction patterns of extracted residue

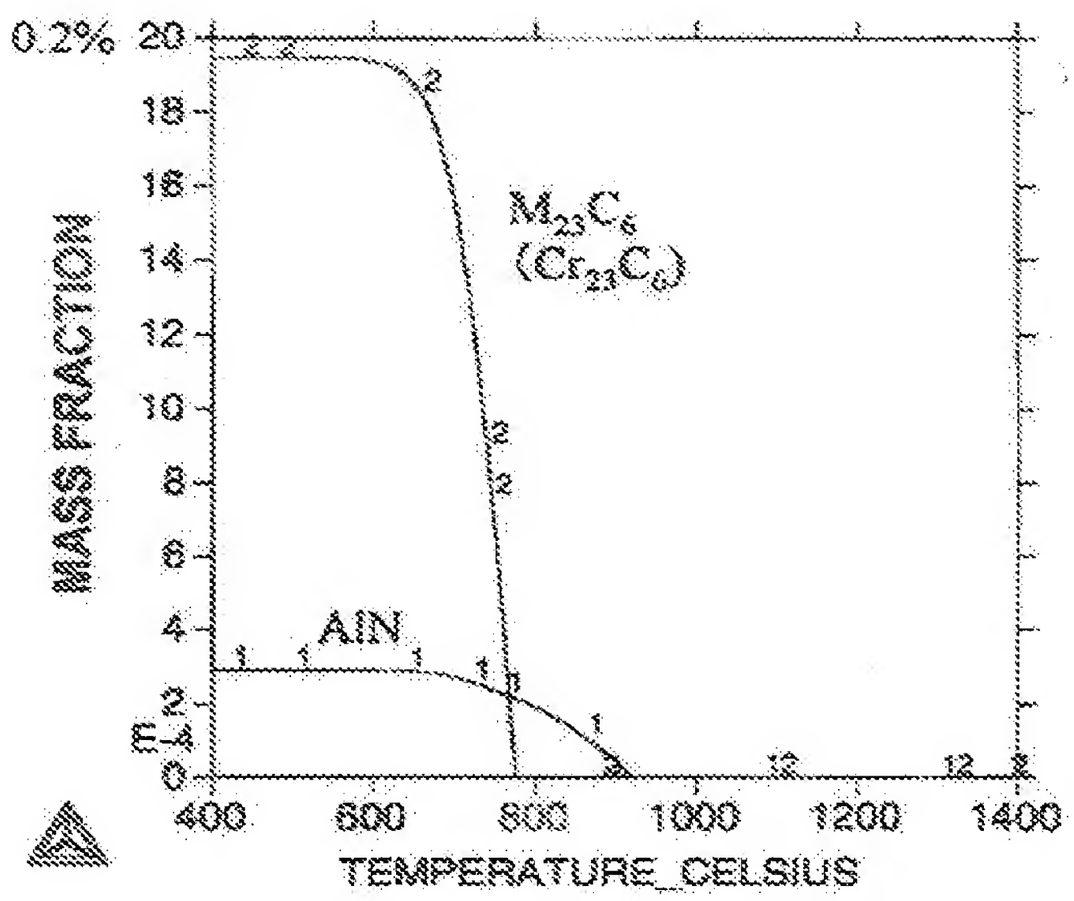

(a) C/0.010, Ti/Less

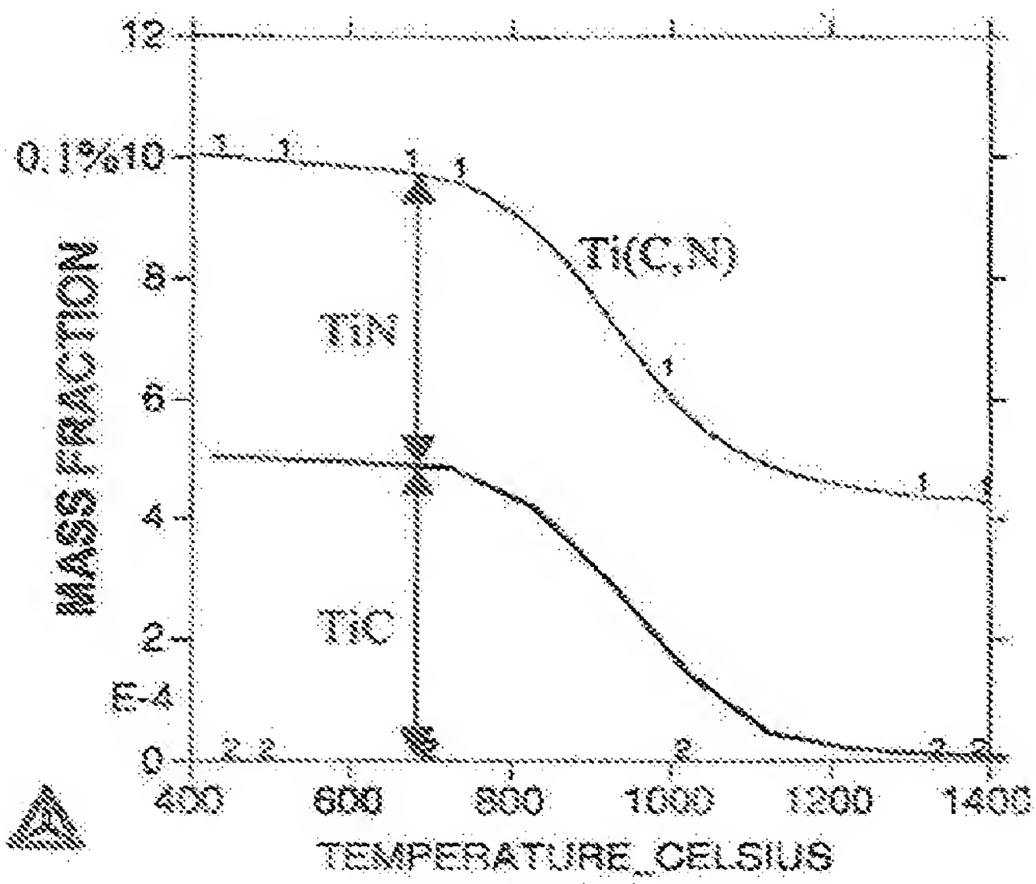

(b) C/0.010, Ti/0.09

FIGURE – 12 Results of thermodynamic calculation for precipitation phase in Ti less and added steels.
(Base compositions: 12Cr-5Ni-2Mo-0.01N)

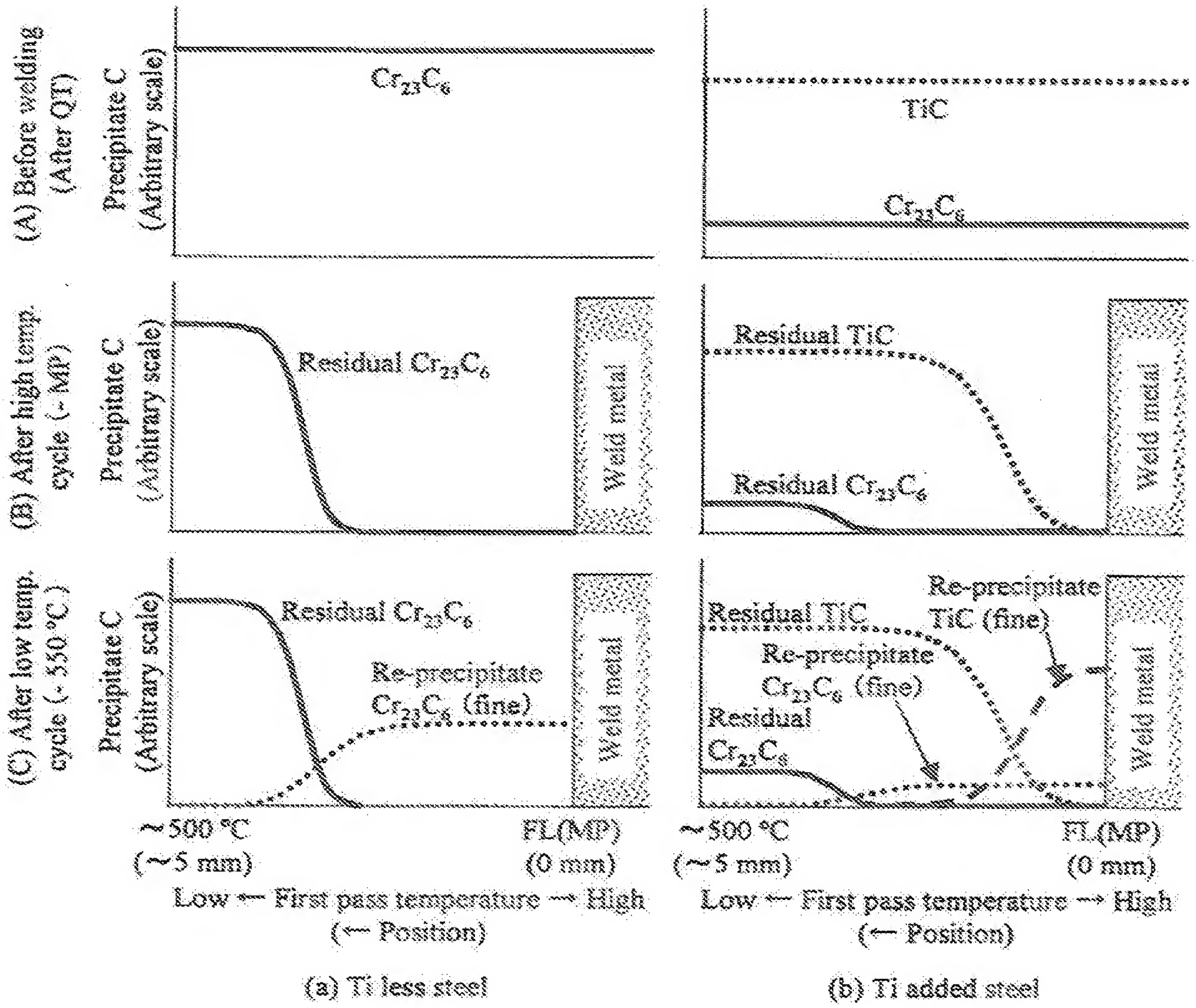

FIGURE – 13 Schematic diagram of carbide precipitation during welding for steels with and without Ti

JFEスチール

13%クロム鋼油井管

世界最大1.2万トン受注

アルジェリア・ガス田開発向け

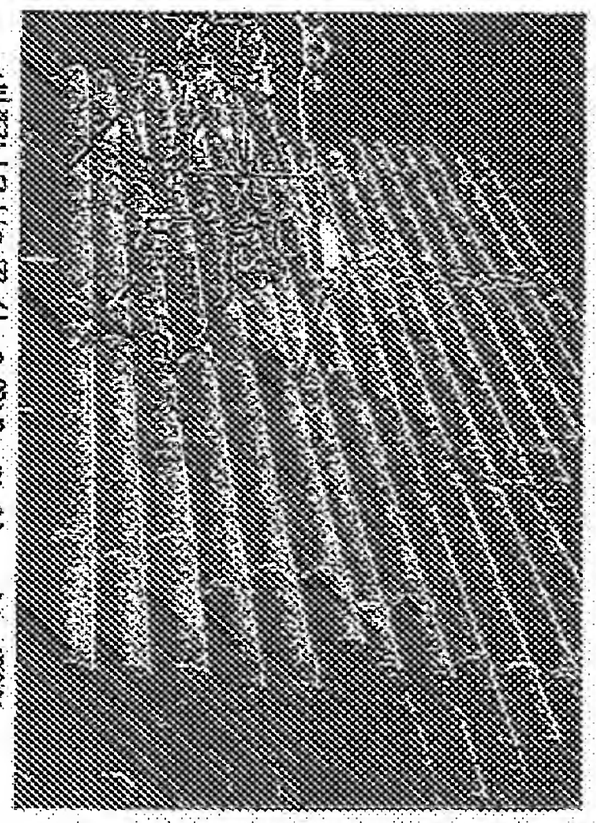

JFEスチールは13%クロム鋼油井管（鋼管）の世界最大1.2万トンの受注に成功した。アルジェリアのイン・サラ・ガス・シュインベンチャー向け。ラインパイプ用13%クロム鋼油井管（シームレス鋼管）の世界最大の受注は2008年、伊藤忠商事が新日鉄と共同で受注したと発表した。1つのプロジェクトにおける、JFEスチールの

2011.9.19 鉄鋼

13%クロム鋼油井管（鋼管）の世界最大1.2万トン受注

アルジェリア・ガス田開発向け

JFEスチールは13%クロム鋼油井管（鋼管）の世界最大の受注に成功した。アルジェリアのイン・サラ・ガス・シュインベンチャー向け。ラインパイプ用13%クロム鋼油井管（シームレス鋼管）の世界最大の受注は2008年、伊藤忠商事が新日鉄と共同で受注したと発表した。1つのプロジェクトにおける、JFEスチールの受注は、2008年の伊藤忠商事、新日鉄の受注（4万5000トン）に次ぐ規模。今後2年間にわたり納入する。

油田の共同開発会社であるイン・サラ・ガス・シュインベンチャーはアルジェリア国営石油会社（ソナトラック社）が55%、スタトイルアルジェリア社が31・55%、BP社が23・15%をそれぞれ出資。油井管は、イン・サラ・ガス油田（埋蔵量：5兆立方メートル）向けのラインパイプ用13%クロム鋼油井管（シームレス鋼管）として受注した。

トータルでスチールは2.2万トンの受注となるが、JFEスチールの受注は、既存ガス田向けなど、今後2年間にわたり納入する。

油井管は、掘削した穴が崩れないようにするケーシングパイプと、原油やガスを地表に運ぶ（生産する）チュービングパイプに分類される。油井管の受注は、JFEスチールの受注は、2008年の伊藤忠商事、新日鉄の受注（4万5000トン）に次ぐ規模。今後2年間にわたり納入する。

油田の共同開発会社であるイン・サラ・ガス・シュインベンチャーはアルジェリア国営石油会社（ソナトラック社）が55%、スタトイルアルジェリア社が31・55%、BP社が23・15%をそれぞれ出資。油井管は、イン・サラ・ガス油田（埋蔵量：5兆立方メートル）向けのラインパイプ用13%クロム鋼油井管（シームレス鋼管）として受注した。

トータルでスチールは2.2万トンの受注となるが、JFEスチールの受注は、既存ガス田向けなど、今後2年間にわたり納入する。

油井管は、掘削した穴が崩れないようにするケーシングパイプと、原油やガスを地表に運ぶ（生産する）チュービングパイプに分類される。油井管の受注は、JFEスチールの受注は、2008年の伊藤忠商事、新日鉄の受注（4万5000トン）に次ぐ規模。今後2年間にわたり納入する。

(Newspaper article)

JFE Steel
13%Cr Stainless Steel Seamless pipe
Receives largest order of maximum 21,000 tons
For gas field development in Algeria

JFE Steel Corporation announced on 18th, acceptance, jointly with Marubeni-Itochu Steel Inc., an order of 21,000 tons of 13%Cr seamless steel pipe for a linepipe for In Salah Gas Joint Venture of Algeria. This order of 13%Cr seamless steel pipe is the largest-ever amount of JFE Steel (3,000 tons is the maximum in the past).

An initial production amount of 2,300 tons has already been shipped and steel pipes of outer diameters of from 6.625 inch (168.3 mm) to 16 inch (406.4 mm) are planned to be shipped in the next 2 years.

The "South Gas Field Development Project of In Salah Gas" handled by the joint venture of development managed by In Salah Gas Joint Venture (amounts of investment: Sonatrach 35%, Statoil 31.05%, BP 33.15%; estimated oil reserve: 7.5 trillion cubic feet) ranks the second in scale in the gas development projects in Algeria. There are included 9 gas fields located in 1,200 km south of the capital city of Algeria and initiated production in 2004.

The 13%Cr seamless steel pipe of JFE Steel is to be used for linepipe connecting the existing gas fields and 4 gas fields,

wherein expansion (long-distance transportation of natural gas) hereafter is planned. The total laying distance of the steel pipe of the project covers 350 km and of which, JFE Steel supplies pipes for 190 km portion. The order of this time has been arrived on the basis of the evaluation of high reliability to past records, including the product quality of 13%Cr seamless steel pipes manufactured by fulfilling vigorous specifications which is required of linepipes. The maximum production of JFE Steel 13%Cr seamless steel pipe amounted to approximately 6,000 tons in 2005.